Document Room, DOCUMENT ROOM 36-412
Research Laboratory of Electronics
Massachusetts Institute of Technology

#3

AXIALLY SYMMETRIC ELECTRON BEAM AND MAGNETIC FIELD SYSTEMS

L. A. HARRIS

LOAN COPY

TECHNICAL REPORT NO. 170

AUGUST 29, 1950

RESEARCH LABORATORY OF ELECTRONICS
MASSACHUSETTS INSTITUTE OF TECHNOLOGY
CAMBRIDGE, MASSACHUSETTS

The research reported in this document was made possible through support extended the Massachusetts Institute of Technology, Research Laboratory of Electronics, jointly by the Army Signal Corps, the Navy Department (Office of Naval Research) and the Air Force (Air Materiel Command), under Signal Corps Contract No. W36-039-sc-32037, Project No. 102B; Department of the Army Project No. 3-99-10-022.

MASSACHUSETTS INSTITUTE OF TECHNOLOGY

RESEARCH LABORATORY OF ELECTRONICS

Technical Report No. 170 August 29, 1950

Axially Symmetric Electron Beam and Magnetic Field Systems

L. A. Harris

This report is identical with a doctoral thesis in the Department of Electrical Engineering, M.I.T.

Abstract

The theory of longitudinally uniform and axially symmetric electron beams focused by a uniform axial magnetic field is presented. It is assumed that the axial velocity is common to all electrons and that they do not cross each other radially. The radial electric, magnetic, and centrifugal forces are balanced if the proper relation between the magnetic field at the cathode and that in the uniform beam is satisfied. This balance is due to the rotation of electrons around the axis brought about by their crossing magnetic field lines. A general graphical method is presented for obtaining the potential distribution required for the design of hollow beams.

The necessity of bringing the beam through a transition region where electrons acquire their angular velocity restricts the problem to two categories in which the cathode is either in a uniform magnetic field or in a magnetically shielded region. Special cases are the solid beam, the hollow beam with uniform radial charge density, the hollow beam between coaxial electrodes at the same potential, and the hollow beam inside an outer electrode only. Of interest is the case of a hollow beam focused with a magnetic field in the cathode region only. Explicit design equations are presented for all cases. The possible effects of incidental ionization are briefly considered.

Experimental results confirm the theory qualitatively and to a considerable extent quantitatively, and indicate the importance of the cathode flux condition and the need for a good method of bringing the beam through the transition region.

I. INTRODUCTION

This paper is a study of the theory and some means for attainment of high-density electron beams of axial symmetry. It is concerned with the general case where a beam with an arbitrary radial charge distribution is made to maintain that distribution over a considerable distance along the axis, and the focusing is brought about by the presence of an axially symmetric magnetic field. Particular attention is paid to hollow electron beams, where the charge density is finite only between two chosen radii, and zero elsewhere.

The interest in this problem is due to the requirements of microwave vacuum tubes, almost all of which make use of an electron beam. These beams differ essentially from those used in more familiar devices, such as the cathode-ray tube, because of their much higher density, the requirement that they remain well-collimated over a long distance, and the requirement that they have a specific and uniform axial velocity.

In the main, only the uniform rod-shaped, or solid, electron beam has been used in tubes like the klystron, traveling-wave tube, and electron-wave tube. Recent developments, though, have indicated that it might be advantageous to use hollow electron beams in certain cases. For instance, a coaxial type waveguiding structure has been suggested for the traveling-wave tube (ref. 1). Also, it is known that in the conventional helix type traveling-wave tube and in the klystron with ungridded resonator gaps, the electrons near the axis of the beam are not efficiently coupled to the fields with which they are supposed to interact. Elimination of this relatively useless core of electrons would decrease greatly the d-c power used in these tubes but would leave the interaction process relatively unchanged. This increase of efficiency due to the use of a hollow beam can be an important factor in the design of high-power microwave tubes.

Although hollow beams are not extensively used at present, their future importance is anticipated here. It is felt that a good understanding of the process of magnetic focusing of dense beams is an important factor in the further advance of the microwave art. Even in the case of solid beams, which are extensively used, the general understanding of the focusing process is not as widespread as it might be. Magnetic focusing is commonly used on an empirical basis. The results are successful but by no means efficient. A great deal of power is wasted in producing magnetic fields much more intense than they need be, if proper design methods were used.

The difficulty in focusing a dense beam over a considerable length is brought about by space-charge repulsion forces. While this problem was recognized and the effects analyzed as early as 1924 (ref. 2), little has been done

about it except to take it into account (ref. 3). As higher density beams came into use the axial magnetic field was applied to keep them collimated. It was pretty clear that such a field would convert any undesired radial velocities into rotational ones and thereby limit the size of the beam. As solid beams only were used, the application of a sufficiently intense magnetic field was sure to limit the variation of beam diameter to within any limits required.

This line of reasoning soon led to the assumption, in many analyses, of infinitely strong fields which confined the electron motion to purely axial trajectories. The properties of both solid and hollow beams in infinitely intense fields have been analyzed (refs. 4 and 5) and these studies are significant in that they clarify the nature of the potential distribution in the beam, and show that there are upper limits on the beam current that can be passed through drift tubes. These infinitely strong fields are never obtained, of course, and so these analyses do have a limited validity. Analyses of the interaction processes in traveling-wave tubes (ref. 6) and klystrons are also based on the assumption of axial electron trajectories, and little thought has been given to the effects of the more complicated trajectories which actually do exist (ref. 7).

Even less thought has been given to the injection of the electron beam into the magnetic field. The solenoidal properties of the magnetic field are too often neglected in this connection.

While certain special instances of magnetic focusing have been treated in the past, notably by Brillouin (refs. 8 and 9), it is only recently that any careful analysis of the subject has been done. The solid electron beam has been treated by Wang (ref. 10) who has shown the role played by the cathode position in the magnetic field. His treatment of the problem is a significant one and forms the basis for much of the analysis presented here. The equilibrium conditions in certain hollow electron beams have been derived by Samuel (ref. 11). The cases treated by him will be shown to be special cases of those developed here.

The purpose of the present investigation is to extend the work of Wang and Samuel in a somewhat more general form with the aim of arriving at practicable design methods which make efficient use of the magnetic field. Although we are concerned primarily with longitudinally uniform electron beams, the cathode position in the magnetic field and other end conditions are so important that considerable attention is paid to them. The aim of deriving design methods for uniform beams governs to a large extent the method of analysis and the restrictions imposed on the problem.

II. THEORY OF INFINITELY LONG BEAMS IN MAGNETIC FIELDS

The development to be carried out in this section is concerned only with the steady-state conditions that can exist in an infinitely long electron beam system. How the beam was produced and placed in the magnetic field is another problem to be considered in a later section.

The only beams of interest here are axially symmetric and longitudinally uniform, so the appropriate coordinate system is the cylindrical one shown in Fig. 1.

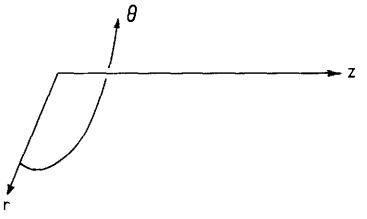

Fig. 1 Cylindrical coordinate system.

It is specified that all electrodes and potentials are independent of θ and z. The magnetic field, too, is axially symmetric, and in the section of the beam being considered, is uniform and in the z direction only.

The velocity range of interest is low enough so that we can neglect relativistic effects, or, what is the same thing, we neglect the magnetic field due to the beam current itself. Every electron is assumed to have started with zero velocity from a cathode at zero potential.

It was indicated at the beginning of this paper that these beams would find application in microwave tubes where the axial velocity is specified. Accordingly, we confine our attention to the one special case where this velocity $\dot{z}$, has the same constant value for every electron in the beam. This is merely one possible mode of existence for the beam; we consider it because it is of the greatest interest and moreover has the advantage of mathematical simplicity.

The two fundamental laws, conservation of energy and conservation of angular momentum, are the basis of this analysis. Conservation of energy gives us the following familiar equation

$$\dot{r}^2 + r^2\dot{\theta}^2 + \dot{z}^2 = -2\frac{e}{m}\varphi \qquad (1)$$

where the dot notation is used to represent total time derivatives; e is the charge on the electron, -16×10^{-20} coulomb; m is the electron mass, 9.1×10^{-31} kilogram; and φ is the electric potential at the point in question as measured from the cathode. All units are MKS rationalized.

The problem to be solved is to determine r as a function of the time t. The solution is obtained as an integral of Eq. 1, but before this is done, the equation must be reduced to one in r alone. Setting $\dot{z}$ equal to a constant has eliminated one variable. It remains to reduce θ and φ to functions of r only.

Reduction of $\dot{\theta}$

The conservation of angular momentum is employed here. In applying this principle, care must be taken to use the correct expression for the angular momentum of a particle in a magnetic field (ref. 8). This is conveniently done by use of the Lagrangian function L (ref. 12).

$$L = -e\varphi + e\bar{A} \cdot \bar{v} + \frac{m}{2}\bar{v} \cdot \bar{v} \tag{2}$$

where $\bar{A}$ is the vector magnetic potential defined by

$$\nabla x\bar{A} = \bar{B}; \tag{3}$$

$\bar{B}$ is the magnetic flux density vector; and $\bar{v}$ is the vector velocity of the particle.

The ith component of momentum is defined by

$$p_i = \frac{\partial L}{\partial \dot{q}_i} \tag{4}$$

where $\dot{q}_i$ is the total time derivative of the ith coordinate of the particle. Defined in this way, p_i is not merely the mechanical momentum mv but depends on $\bar{A}$ also. The equations of motion are found by means of Euler's equation (ref. 12).

$$\frac{d}{dt}\left(\frac{\partial L}{\partial \dot{q}_i}\right) - \frac{\partial L}{\partial q_i} = 0 . \tag{5}$$

The vector $\bar{v}$ is represented in the cylindrical coordinate system by

$$\bar{v} = \bar{i}_r\dot{r} + \bar{i}_\theta r\dot{\theta} + \bar{i}_z\dot{z} \tag{6}$$

where the i_i are unit vectors.

The axially symmetric magnetic fields may be produced by currents flowing in the θ direction and the vector potential $\bar{A}$ has a θ component, A_θ, only.

Substitution of (6) into (2) yields

$$L = -e\varphi + eA_\theta r\dot{\theta} + \frac{m}{2}(\dot{r}^2 + r^2\dot{\theta}^2 + \dot{z}^2) \tag{7}$$

and Euler's Eq. 5 for the θ component gives

$$eA_\theta r + mr^2\dot{\theta} = \text{constant}. \tag{8}$$

Equation 8 is an explicit statement of the conservation of angular momentum. We used the Lagrangian and the vector potential because of the simplicity of the method and the ability to express the magnetic field with a single component of $\bar{A}$. The constant may be evaluated for any one electron by considering the conditions at the cathode at the starting point of that electron. Here the constant is $eA_c r_c + mr_c^2\dot{\theta}_c$ where the subscript c refers to the conditions at the cathode. We have already assumed that the electron

velocity here is zero, hence the tangential velocity $r_c\dot{\theta}_c$, in particular, is zero. Consequently, $eA_\theta r + mr^2\dot{\theta} = eA_c r_c$ or

$$\dot{\theta} = \frac{e/m}{r^2}(r_c A_c - rA_\theta) \quad . \tag{9}$$

The physical meaning of this result is more evident when the equation is put into terms of magnetic flux rather than vector potential. Consider two circles coaxial with the beam, one of radius r, passing through the position of the electron, the other of radius r_c passing through the starting point of this electron. These circles are shown in Fig. 2. On either of them Stoke's theorem may be applied.

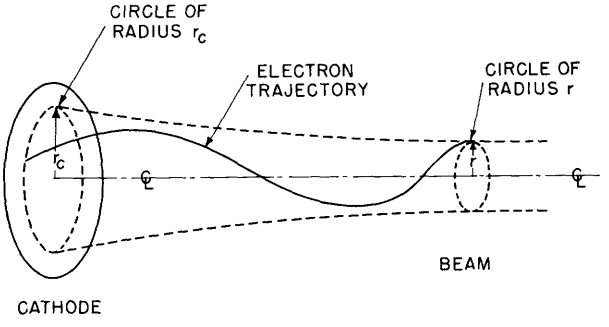

Fig. 2 Illustrating the meaning of Ψ and ψ_c.

$$\iint_S (\nabla \times \bar{A}) \cdot d\bar{s} = \oint \bar{A} \cdot d\bar{l} \quad . \tag{10}$$

The surface integral is taken over the area of the circle while the line integral is taken around its perimeter. By symmetry

$$\oint \bar{A} \cdot d\bar{l} = 2\pi r A_\theta \tag{11}$$

and since $B = \nabla \times \bar{A}$

$$\iint_S (\nabla \times \bar{A}) \cdot d\bar{s} = \iint_S \bar{B} \cdot d\bar{s} = \psi \tag{12}$$

where ψ is the magnetic flux linking the circle. If ψ_c denotes the flux linking the cathode circle, we may rewrite (9) as follows

$$\dot{\theta} = \frac{e/m}{2\pi r^2}(\psi_c - \psi) \quad . \tag{13}$$

The derivation of this result, known as Busch's Theorem (ref. 13), has been included here for the sake of clarity and completeness, though it may be found elsewhere (refs. 10 and 11).

Since the magnetic field is assumed to be known and time invariant, it is evident that (13) expresses the angular velocity as a function of position only. If the magnetic field is uniform, then $\dot{\theta}$ is a function of r only. The field need be uniform, however, only in the region of the electron's present position for this dependence of $\dot{\theta}$ on r alone to be true. At the cathode or any other intermediate region the field may be nonuniform though it must be axially symmetric.

Reduction of φ

In order to reduce φ to a function of r only, we assume that electrons do not cross each other radially in the course of their travel down the tube. The beam is symmetrical so we can think of cylindrical shells of electrons which make up the beam. These shells may vary in radius along the length of the

beam, but they are assumed never to intersect one another or trade positions. This assumption, which appears to be a radical one is necessary for a convenient solution to the problem. The principal reason for its use is mathematical simplicity, although there is some justification for it aside from this.

If we were to solve this problem exactly we should have to calculate the trajectory of each electron using the potential it experiences due to the electrodes and to all the other electrons. But each of these other electrons has its own trajectory which in turn depends on all others. The task is clearly impossible. At this point we take advantage of the fact that we know what type of solution we are seeking.

Our object is to learn how to obtain beams in which the electrons do not have much radial motion. If they do, then we are not interested in that beam. For the type of beam we are trying to achieve the potential is closely approximated by that of a uniform beam which is in radial equilibrium.

If we use the potential of such a uniform beam and still allow for some radial motion, we are in effect using an average potential $\bar{\varphi}$, and neglecting any longitudinal electric fields due to variations in beam diameter.

We cannot use $\bar{\varphi}$ directly in Eq. 1 either. This procedure would assume that the entire beam stayed in equilibrium while the electron in question threaded its way in and out of the beam. The solution obtained in such a manner would have to indicate a beam with no changes in radius in order to be consistent. By assuming that electrons do not cross radially, we are enabled to use the average potential $\bar{\varphi}$ and still allow for radial variations in the entire beam. The assumption is clearly true for a beam in equilibrium and is probably a fair approximation in beams with only small variations from equilibrium. It will be shown to be true also in certain other instances.

According to the assumption, each electron shell encloses a constant amount of charge which may be considered to lie along the axis. This line charge produces a logarithmic potential around it. It is therefore possible to express the potential φ as experienced by the electrons in any one shell as

$$\varphi = \alpha \ln \frac{r}{r_o} + \gamma \qquad (14)$$

where r_o is the radius at which the electrons of that shell experience no radial force, their equilibrium radius. The coefficients α and γ are constants for any one shell, but vary from shell to shell. We shall characterize the electron shells by their equilibrium radius r_o. The coefficients α and γ are thus functions of r_o, but not of r or t. They are evaluated by means of their relationship to the average potential $\bar{\varphi}$. When the beam is in equilibrium φ and $\bar{\varphi}$ must be equivalent and so must their derivatives with respect to r.

$$[\varphi]_{r_o} = [\bar{\varphi}]_{r_o}$$
$$\left[\frac{\partial\varphi}{\partial r}\right]_{r_o} = \left[\frac{\partial\bar{\varphi}}{\partial r}\right]_{r_o} \qquad (15)$$

These equations are used to determine α and γ and this operation is carried out in the next section after the calculation of $\bar{\varphi}$ itself. The expression for φ given in (14) is not the true potential but it is the potential experienced by the electron and is used in (1) to solve for the trajectories.

At r_o, φ becomes γ, so γ is the average potential at r_o, while α is a coefficient giving the magnitude and direction of the radial electric field.

Equilibrium and Stability Conditions

Now that $\dot{\theta}$ and φ have been reduced to functions of r we can substitute them into Eq. 1 to obtain a differential equation in r only.

$$\dot{r}^2 + r^2\left[\frac{e/m}{2\pi r^2}(\psi_c - \psi)\right]^2 + \dot{z}^2 = -2\frac{e}{m}\left[\alpha \ln\frac{r}{r_o} + \gamma\right] \qquad (16)$$

As $\dot{z}$ is the same constant for all electrons it corresponds to an accelerating voltage V defined by

$$\dot{z}^2 = -2\frac{e}{m}V \qquad (17)$$

Equation 16 becomes

$$\dot{r}^2 = -2\frac{e}{m}\alpha \ln\frac{r}{r_o} - 2\frac{e}{m}(\gamma - V) - \left(\frac{e/m}{2\pi r}\right)^2(\psi_c - \psi)^2. \qquad (18)$$

In the region of the beam that we are studying, the magnetic field is axial and uniform as required by the reduction of $\dot{\theta}$. Since the field has only a z component B_z, it will be permissible to denote it simply by B without fear of confusion. The flux ψ is given by

$$\psi = \pi r^2 B \qquad (19)$$

and the flux ψ_c linking the cathode circle is a constant depending only on r_o. If we let

$$\omega_H = \frac{e}{m}\frac{B}{2} \qquad (20)$$

and

$$\Omega = \frac{e}{m}\frac{\psi_c}{2\pi} \qquad (21)$$

then after expansion and substitution of the last three equations, (18) becomes

$$\dot{r}^2 = -2\frac{e}{m}\alpha \ln\frac{r}{r_o} - 2\frac{e}{m}(\gamma - V) - \frac{\Omega_2}{r^2} - \omega_H^2 r^2 + 2\Omega\omega_H \qquad (22)$$

This is the differential equation of radial motion of any electron in the beam.

Equation 22 may be interpreted as defining a potential trough in which the electron rides. The kinetic energy associated with radial motion is $m/2\ \dot{r}^2$. As Eq. 1 defines the total energy as zero, the negative of $m/2\ \dot{r}^2$ may be considered as a potential energy, so far as radial motion is concerned. This is merely an arbitrary division of the total energy into potential and kinetic terms, but it is a convenient aid in visualizing the radial motion (ref. 10).

The right-hand side of (22) becomes minus infinity for r approaching either zero or infinity regardless of whether α is positive or negative. Only the region in which this quantity is greater than zero is accessible to the electron in question. The magnetic field, by limiting the energy of radial motion, prevents electrons from traveling arbitrarily far from or close to the axis.

Taking the time derivative of (22) and dividing by $2\dot{r}$ gives us the equation for the radial acceleration.

$$\ddot{r} = -\frac{e}{m}\frac{\alpha}{r} + \frac{\Omega^2}{r^3} - \omega_H^2 r \ . \tag{23}$$

We have defined r_o as the radius at which there is no radial force, hence $\ddot{r} = 0$ at $r = r_o$.

$$0 = -\frac{e}{m}\frac{\alpha}{r_o} + \frac{\Omega^2}{r_o^3} - \omega_H^2 r_o \ . \tag{24}$$

Solution for Ω yields

$$\Omega = \omega_H r_o^2 \sqrt{1 + \frac{e/m}{\omega_H^2 r_o^2}\,\alpha} \tag{25}$$

where only the positive square root is intended here and elsewhere in this paper. The negative root would indicate a reversal of direction of magnetic field between the cathode and the beam. Although this is possible, most practical configurations will not have this reversal.

It is convenient to let

$$\frac{e/m}{\omega_H^2 r_o^2} = K \tag{26}$$

so that the flux condition may be written

$$\Omega = \omega_H r_o^2 \sqrt{1 + K\alpha}$$

or

$$\psi_c = \pi r_o^2 B \sqrt{1 + K\alpha} \ . \tag{27}$$

K is a negative number because of the negative electron charge. The quantity $\sqrt{1 + K\alpha}$ is less than or greater than one depending on whether α is greater than or less than zero respectively. If α is positive, the electric force

tends to move electrons toward increasing radii. In this case, for ψ_c to be real, $K\alpha$ must be greater than -1. Presently we shall see that this condition guarantees that the radial motion shall be periodic; i.e. stable.

Equation 27 shows that the flux ψ_c linking the cathode circle is less than the flux ψ linking the equilibrium circle of radius r_o (see Fig. 2) if the electric force is outward. This is always the case with solid beams and may be true with hollow beams too. If the electric force is inward, a condition which can occur only when there is an electrode inside a hollow beam, the cathode flux ψ_c must be greater than ψ.

The electron motion will be a stable oscillation about r_o if the equivalent potential energy is a minimum at r_o, or if $\ddot{r}$ is negative for r greater than r_o, and positive for r less than r_o. To check the stability of the motion, we take the derivative of (23) with respect to r and evaluate it at $r = r_o$.

$$\left[\frac{\partial \ddot{r}}{\partial r}\right]_{r_o} = \frac{e}{m}\frac{\alpha}{r_o^2} - 3\frac{\Omega^2}{r_o^4} - \omega_H^2 \quad . \tag{28}$$

Substitution of (24) into (28) yields

$$\left[\frac{\partial \ddot{r}}{\partial r}\right]_{r_o} = -2\frac{e}{m}\frac{\alpha}{r_o^2} - 4\,\omega_H^2 \quad . \tag{29}$$

As the left-hand side of (29) must be negative, dividing the right-hand side by $-4\,\omega_H^2$ shows that the following inequality must be true.

$$1 + \frac{K\alpha}{2} > 0$$

or

$$K\alpha > -2 \quad . \tag{30}$$

In any physical arrangement, however, ψ_c must be real so that the above inequality is always satisfied. An unstable radial oscillation of the beam in the presence of a magnetic field is not possible. The instability encountered in a beam in a field-free space may be considered as the beginning of an oscillation about r_o, where r_o has moved out to infinity because ω_H is zero and K remains finite.

The above considerations of equilibrium conditions show that any general radial charge distribution is a possible stable configuration so long as the proper flux condition (27) and stability condition (30) are satisfied. This conclusion is demonstrated in an alternative way, and perhaps more explicitly, by a variational treatment of the problem presented in an appendix.

Solution of the Differential Equation

In order to solve the equation of motion (22), we make the following

changes

$$r^2 = R$$

and (31)

$$r_o^2 = R_o$$

then

$$\dot{R} = 2\, r\dot{r}$$

and (32)

$$\ddot{R} = 2\, r\ddot{r} + 2\dot{r}^2 \ .$$

We multiply (22) by 2, (23) by 2r and add the results to obtain

$$\ddot{R} = \left[-2\frac{e}{m}\alpha - 4\frac{e}{m}(\gamma - V) + 4\Omega\omega_H\right] - 2\frac{e}{m}\alpha \ln\frac{R}{R_o} - 4\omega_H^2 R \ . \qquad (33)$$

The presence of the logarithmic term in (33) makes it a nonlinear differential equation. It can be solved approximately, however, by using the first term of the series expansion for $\ln R/R_o$

$$\ln\frac{R}{R_o} \approx \frac{R}{R_o} - 1 \ . \qquad (34)$$

As (34) is true only for values of R/R_o close to one, our solution will be valid in this range only. Fortunately it is the range in which we are primarily interested. (For $R/R_o = 1.2$, or $r/r_o = 1.095$, the error is about 10 per cent in (34).)

With this last substitution (33) simplifies to the linear equation

$$\ddot{R} = a_o + a_1 R \qquad (35)$$

where

$$a_o = \left[-4\frac{e}{m}(\gamma - V) + 4\Omega\omega_H\right] = 4\omega_H^2 r_o^2\left[\sqrt{1 + K\alpha} - K(\gamma - V)\right]$$

and

$$a_1 = -\left(4\omega_H^2 + 2\frac{e}{m}\frac{\alpha}{r_o^2}\right) = -4\omega_H^2\left(1 + \frac{K\alpha}{2}\right) \ .$$

We multiply (35) by $2\dot{R}$ and integrate once.

$$2\dot{R}\ddot{R} = 2a_o\dot{R} + 2a_1 R\dot{R}$$

$$\dot{R}^2 = 2a_o R + a_1 R^2 + a_2 \ . \qquad (36)$$

The constant of integration, a_2, is evaluated by substituting (22) into (36) and setting $r = r_o$. This procedure gives

$$a_2 = -4\omega_H^2 R_o^2\left(1 + \frac{K\alpha}{2}\right) \ . \qquad (37)$$

The integral of (36) neglecting the additive phase constant is

$$R = b_o + b_1 \cos \beta t \ . \tag{38}$$

Differentiating (38) with respect to time and using the identity

$$\cos^2 \beta t + \sin^2 \beta t = 1$$

enables us to evaluate b_o, b_1, and β. The results are

$$\beta = -2\omega_H \sqrt{1 + \frac{K\alpha}{2}}$$

$$b_o = R_o \left[\frac{\sqrt{1 + K\alpha} - K(\gamma - V)}{1 + \frac{K\alpha}{2}} \right] \tag{39}$$

$$b_1 = R_o \sqrt{(b_o/R_o)^2 - 1} \ .$$

The final solution for the radius of any electron in the beam as a function of time, valid only for small oscillations, may be written

$$\frac{R}{R_o} = \left[\frac{\sqrt{1 + K\alpha} - K(\gamma - V)}{1 + \frac{K\alpha}{2}} \right] + \left\{ \left[\frac{\sqrt{1 + K\alpha} - K(\gamma - V)}{1 + \frac{K\alpha}{2}} \right]^2 - 1 \right\}^{\frac{1}{2}} \cos\left(-2\omega_H \sqrt{1 + \frac{K\alpha}{2}}\ t\right) \tag{40}$$

If we introduce a new quantity x, defined by

$$\frac{b_o}{R_o} = 1 + \frac{x^2}{2} \tag{41}$$

then (40) may be written in the neater form

$$\frac{R}{R_o} = 1 + \frac{x^2}{2} + x \sqrt{1 + \frac{x^2}{4}} \cos \beta t \ . \tag{42}$$

It is apparent from (42) that as the normalized amplitude of oscillation increases so does the average radius about which this motion takes place. Figure 3 is a graph of the maximum and minimum values of R/R_o vs. the magnitude of the amplitude factor x. The oscillation is displaced toward the outside of R_o, the unbalance increasing with the amplitude of oscillation.

A significant point in the solution is the form of the angular frequency of radial oscillation

$$\beta = -2\omega_H \sqrt{1 + \frac{K\alpha}{2}} \ .$$

For stable solutions β must be real as specified by (30), and since ψ_c is real, this is always the case.

Figure 4 is a graph showing the general form of β as a function of $-\omega_H$ which is proportional to the magnetic flux density B.

When α is positive and the electric force on the particles is outward, there is a minimum magnetic field below which the oscillation is not stable.

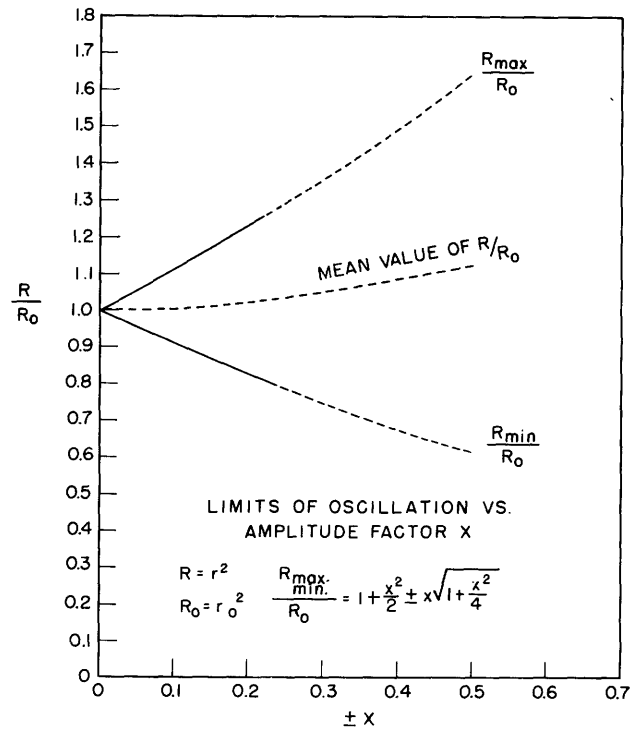

Fig. 3 Maximum and minimum radii vs. amplitude factor.

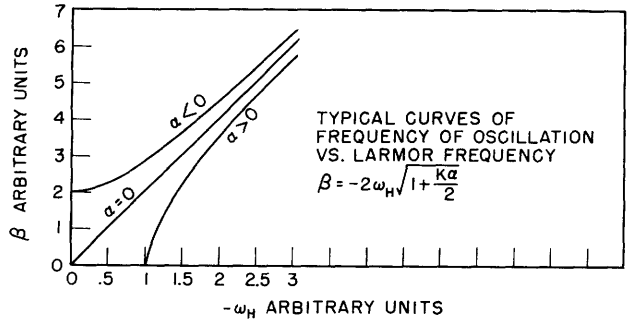

Fig. 4 Oscillation frequency vs. magnetic field.

When there is no electric force in the radial direction ($\alpha = 0$), the beam is in equilibrium when there is no magnetic field and it oscillates when there is a magnetic field. But when α is negative, β remains real even though the magnetic field becomes zero. It is thus possible, by means of an inward electric force, to have a stable configuration of the beam with no magnetic field along its length. This case is of considerable practical significance as it allows a great saving in power used to produce the magnetic field. It is discussed in some detail in a later section, as one case of special interest.

It is necessary to check the form of β with the assumption made in deriving it. The only questionable part of this development was the statement that electrons do not cross each other radially. This assumption has certain consequences not pointed out previously, but readily appreciated when one examines the behavior of two adjacent electron shells.

If one shell oscillates in radius along the length of the beam, then the other must do likewise, or they will intersect. The space periods or wavelengths of these oscillations, moreover, must be the same for both shells, and the phases must be the same; when one shell expands, so must the other. A simple extension of these considerations leads us to the restriction that the angular frequency β must be the same for all shells, hence independent of r_o or of R_o. This, clearly, is not the case unless $K\alpha$ is independent of r_o, or α is proportional to r_o^2. When this is true, the solution is entirely consistent with our assumptions. This point will be discussed also in later sections, particularly the one dealing with special cases.

The assumption of noncrossing also requires that the amplitude of oscillation be a continuous function of r_o. Though not necessarily so, this function may be monotonic with a zero value entirely inside the beam, somewhere in the charge region, or entirely outside the beam. If either the first or last possibility is true, the beam oscillates more or less as a unit, with the inside and outside edges moving in and out together. If the amplitude is zero for a value of r_o in the charge region, then the beam pulsates in thickness, the outside expanding while the inside contracts.

Although the solution we have found is not generally consistent with the assumption of noncrossing, it is conceivable that the results may still be useful. We shall always try to satisfy the equilibrium conditions in any design. With little or no oscillation there will not be much crossing and our results may be sufficiently accurate to be useful.

It is possible too that the variation of space period across the beam will be small so that interference of the electron paths may not develop until many cycles have elapsed. In the entire length of the beam there may not be any serious radial crossing. While these considerations may give us hope for the usefulness of the general solution, its real test must come with experiment.

There is one other possibility for consistent solutions as derived here. If the axial velocity is allowed to assume different values for different electron shells, then the time period may vary while the space period remains the same for all shells. In this paper, however, we are concerned only with the case where $\dot{z}$ and V are the same for all shells.

Angular Velocity

A consideration of the angular velocity is helpful in clarifying the physical picture of the focusing process. We return to Eq. 13

$$\dot{\theta} = \frac{e/m}{2\pi r^2} \left(\psi_c - \psi\right)$$

and the earlier definitions of Ω and ω_H (Eqs. 20 and 21) to obtain

$$\dot{\theta} = \frac{\Omega}{r^2} - \omega_H \,. \tag{43}$$

We substitute (27) into (43) to get

$$\dot{\theta} = \omega_H \left(\frac{r_o^2}{r^2} \sqrt{1 + K\alpha} - 1 \right) \tag{44}$$

and finally, use of Eq. 42 leaves us with

$$\dot{\theta} = \omega_H \left[\frac{\sqrt{1 + K\alpha}}{1 + \frac{x^2}{2} + x\sqrt{1 + \frac{x^2}{4}} \cos \beta t} - 1 \right] \tag{45}$$

Evidently $\dot{\theta}$ is a periodic quantity. If $\sqrt{1+K\alpha}$ is sufficiently small, the sign of $\dot{\theta}$ alternates, otherwise $\dot{\theta}$ fluctuates in value but retains the same sign.

The average value of $\dot{\theta}$ is of interest. This is given by

$$\bar{\dot{\theta}} = \frac{1}{2\pi}\int_0^{2\pi} \dot{\theta}\, d(\beta t) = \frac{\omega_H\sqrt{1+K\alpha}}{2\pi(1+\frac{x^2}{2})}\int_0^{2\pi} \frac{d(\beta t)}{1+\frac{x\sqrt{1+x^2/4}}{1+x^2/2}\cos\beta t} - \omega_H \,. \tag{46}$$

Or integration, (46) becomes

$$\bar{\dot{\theta}} = \omega_H(\sqrt{1+K\alpha} - 1) \,. \tag{47}$$

The form of the average angular velocity explains the focusing action. The sign of $\bar{\dot{\theta}}$ is the same as the sign of α, since both K and ω_H are numerically negative. If the electric force on an electron is outward, it encircles the axis in such a direction as to produce an inward magnetic force, and vice versa. This average rotation is independent of x and its magnitude depends only on the relative values of electric and magnetic fields. It is the familiar Larmor precession or drift. The oscillations in radius and in angular velocity represent a motion similar to the trochoids and cycloids experienced in uniform crossed electric and magnetic fields. These paths are shown in Fig. 5. Which type of path the electrons follow is determined by the relative values of $\sqrt{1+K\alpha}$ and x.

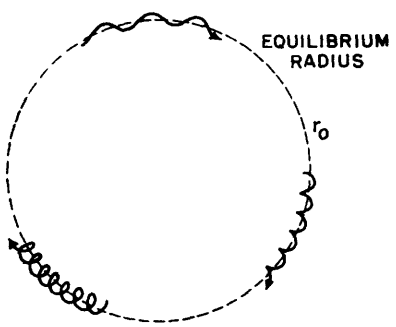

Fig. 5 The three possible electron trajectories.

Since $\bar{\dot{\theta}}$ is a function of $K\alpha$ which is not generally independent of r_o, there is a rotational shearing motion between different electron shells, aside from the oscillatory rotation. This slipping of the shells does not introduce any complication of the picture because of the axial symmetry. In the consistent case where α is proportional to r_o^2, the entire beam rotates as a unit.

The energy balance of the system is another point of interest. The kinetic energy of any particle is divided between axial, radial and angular velocities. At the equilibrium radius r_o, the potential φ is equal to γ so the total kinetic energy must be $-e\gamma$. The energy associated with the axial velocity is $-eV$, and the difference, $-e(\gamma - V)$ is associated with the angular and radial velocities. Clearly $\gamma - V$ must be a positive quantity, a conclusion borne out by the coefficients appearing in Eq. 40.

This energy difference has a minimum possible value that it must have to

account for the angular velocity which in turn is specified solely by the magnetic field configuration. Any excess over this minimum means a certain amount of radial motion. The design procedure consists of setting $\gamma - V$ equal to this minimum as we shall see in the section dealing with the design of the beam system.

Before we go on to consider this question, it is necessary to examine the electric potential distribution in the beam and to evaluate the coefficients α and γ. This is the subject of the following section.

III. THE ELECTRIC POTENTIAL IN THE BEAM

In sec. II it was explained that the potential φ as experienced by the electrons could be expressed in the form $\varphi = \alpha \ln r/r_0 + \gamma$. It was also pointed out that in order to determine the coefficients α and γ, it is necessary to calculate the average potential $\bar{\varphi}$ corresponding to a beam system uniform in the axial direction. This section is concerned with these calculations and their application to the problem.

The system under consideration is axially symmetric and uniform longitudinally. The only variations that take place are in the radial direction. As the most general case we assume a hollow electron beam, coaxial with two cylindrical electrodes, one inside the beam, the other outside. As shown in Fig. 6, φ_1 is the actual potential, as measured from the cathode, applied to the inner electrode of radius r_1. The quantities φ_2 and r_2 are similarly connected with the outer electrodes; the subscripts a and b refer to the inner and outer edges of the beam respectively.

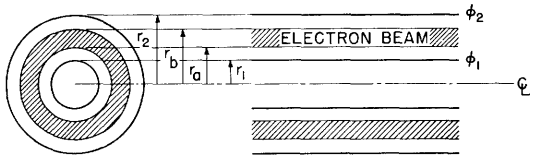

Fig. 6 Hollow beam in equilibrium.

The charge density in the beam is a function of radius only and is denoted by ρ. Its general form is

$$\begin{aligned} \rho &= \rho(r) && r_a \leq r \leq r_b \\ &= 0 && r < r_a \text{ or } r_b < r \,. \end{aligned} \tag{48}$$

Equation 48 represents a hollow beam, but can be made to represent a solid one by letting r_a become zero. In that case the inner electrode must disappear and we need not concern ourselves with φ_1. In the same way, the inner electrode may be removed by letting r_1 become zero even if the beam remains hollow, and the outer electrode may be removed by letting r_2 recede to infinity.

The charge density $\rho(r)$, being a physical quantity, is an analytic

function with no singularities in the region with which we are concerned ($r_a \leq r \leq r_b$). We may, therefore, expand ρ as a power series about some point in the beam say r_o, ($r_a \leq r \leq r_b$). In the charge region only, therefore

$$\rho(r) = \sum_{n=0}^{\infty} \rho_n' (r_o - r)^n . \tag{49}$$

Because $\rho(r)$ is a physical quantity, the series of (49) is absolutely convergent in this range, so it may be expanded and rearranged into the form

$$\rho(r) = \sum_{n=0}^{\infty} \rho_n r^n \tag{50}$$

where only positive integral values of n occur. Note that only ρ_o has the dimensions of charge density while ρ_n has the dimensions charge density/ length^n.

The evaluation of $\bar{\varphi}$ consists of integrating Poisson's equation

$$\frac{1}{r} \frac{\partial}{\partial r} \left(r \frac{\partial \bar{\varphi}}{\partial r}\right) = -\frac{\rho}{\varepsilon} \tag{51}$$

where ε is the permittivity of free space, ($1/36\pi \times 10^{-9}$ farads/meter), and matching the solution to the boundary conditions at r_1 and r_2. To do this, we follow Wang (ref. 10) by letting

$$\bar{\varphi} = \varphi_s + \varphi_L \tag{52}$$

where φ_s is a solution of (51) and φ_L is a solution of Laplace's equation

$$\frac{1}{r} \frac{\partial}{\partial r} \left(r \frac{\partial \varphi_L}{\partial r}\right) = 0 . \tag{53}$$

The sum of these two solutions must also be a solution of (51). By means of this separation we determine the individual contributions to the potential $\bar{\varphi}$ of the charge in the beam, and of the charge on the electrodes. In the following we shall indicate the formal process in this calculation and then give the results which are obtained when these operations are performed on the power series represented in (50).

The potential φ_s due to space-charge alone is evaluated first. From (51) we have

$$\frac{\partial}{\partial r} \left(r \frac{\partial \varphi_s}{\partial r}\right) = -\frac{\rho}{\varepsilon} r .$$

Since ρ is zero for values of r less than r_a, we need integrate only from r_a outward. The upper limit of integration is just r, a variable radius lying somewhere in the charge region.

$$r \frac{\partial \varphi_s}{\partial r} = -\frac{1}{\varepsilon} \int_{r_a}^{r} \rho r dr . \tag{54}$$

Only one term appears on the left since this component of the electric field is zero everywhere inside the charge ring.

Integrating (54) once more gives us the potential φ_s for any value of r lying in the charge ring.

$$\varphi_s = - \int_{r_a}^{r} \left[\frac{1}{\varepsilon r} \int_{r_a}^{r} \rho r dr \right] dr \ . \tag{55}$$

This time only φ_s appears on the left because we have arbitrarily chosen $\varphi_s = 0$ inside r_a.

Before we can evaluate φ_L, we shall have to calculate the contribution of φ_s at the outer electrode, i.e. at r_2. At the outer edge of the electron beam we have, from (55)

$$\varphi_{s_b} = - \int_{r_a}^{r_b} \left[\frac{1}{\varepsilon r} \int_{r_a}^{r} \rho r dr \right] dr \ . \tag{56}$$

Outside the electron beam, the potential φ_s is represented by the familiar logarithmic expression due to a line charge along the axis.

$$\varphi_s = - \frac{Q}{2\pi\varepsilon} \ln \frac{r}{r_b} + \varphi_{s_b} \ , \ r > r_b \tag{57}$$

where Q is the total charge in the beam per unit length.

$$Q = 2\pi \int_{r_a}^{r_b} \rho r dr \ . \tag{58}$$

The potential φ_s can now be written for the radius r_2, by substituting (58) and (56) into (57).

$$\varphi_{s_2} = - \frac{1}{\varepsilon} \int_{r_a}^{r_b} \left[\rho r \ln \frac{r_2}{r_b} + \frac{1}{r} \int_{r_a}^{r} \rho r dr \right] dr \ . \tag{59}$$

Since $\varphi_2 = \varphi_{L_2} + \varphi_{s_2}$, we have that

$$\varphi_{L_2} = \varphi_2 + \frac{1}{\varepsilon} \int_{r_a}^{r_b} \left[\rho r \ln \frac{r_2}{r_b} + \frac{1}{r} \int_{r_a}^{r} \rho r dr \right] dr \tag{60}$$

and

$$\varphi_{L_1} = \varphi_1 \tag{61}$$

because we have set $\varphi_{s_1} = 0$ in Eq. 55. The solution for φ_L is well known and has the following form

$$\varphi_L = \frac{\varphi_{L_2} - \varphi_{L_1}}{\ln \frac{r_2}{r_1}} \ln \frac{r}{r_1} + \varphi_{L_1} \ . \tag{62}$$

This equation, which applies everywhere between r_1 and r_2, becomes

$$\varphi_L = \frac{\varphi_2 - \varphi_1 + \frac{1}{\varepsilon}\int_{r_a}^{r_b}\left[\rho r \ln\frac{r_2}{r_b} + \frac{1}{r}\int_{r_a}^{r}\rho r dr\right]dr}{\ln\frac{r_2}{r_1}} \ln\frac{r}{r_1} + \varphi_1 \qquad (63)$$

when (60) is substituted into it.

Finally, the resultant potential, for any radius r in the charge region, i.e. for $r_a \leq r \leq r_b$ is given by the sum of (55) and (63).

$$\bar{\varphi} = \frac{\varphi_2 - \varphi_1 + \frac{1}{\varepsilon}\int_{r_a}^{r_b}\left[\rho r \ln\frac{r_2}{r_b} + \frac{1}{r}\int_{r_a}^{r}\rho r dr\right]dr}{\ln\frac{r_2}{r_1}} \ln\frac{r}{r_1}$$

$$+ \varphi_1 - \frac{1}{\varepsilon}\int_{r_a}^{r}\left[\frac{1}{r}\int_{r_a}^{r}\rho r dr\right]dr . \qquad (64)$$

We shall find it convenient to denote the coefficient of the logarithmic term, which is a constant of the system, by a shorter symbol, a. Thus

$$\varphi = a \ln\frac{r}{r_1} + \varphi_1 - \frac{1}{\varepsilon}\int_{r_a}^{r}\left[\frac{1}{r}\int_{r_a}^{r}\rho r dr\right]dr . \qquad (65)$$

With (50) substituted into it,

$$a = \frac{\varphi_2 - \varphi_1 + (\ln r_2/r_b)\frac{Q}{2\pi\varepsilon} + \frac{1}{\varepsilon}\sum_0^\infty \frac{\rho_n}{(n+2)^2}(r_b^{n+2} - r_a^{n+2}) - \frac{1}{\varepsilon}\sum_0^\infty \frac{\rho_n r_a^{n+2}}{n+2}\ln\frac{r_b}{r_a}}{\ln\frac{r_2}{r_1}}$$

This equation may be further simplified by integrating the last term by parts, which gives us

$$\bar{\varphi} = a \ln\frac{r}{r_1} + \varphi_1 - \frac{1}{\varepsilon}\ln\frac{r}{r_a}\int_{r_a}^{r}\rho r dr + \frac{1}{\varepsilon}\int_{r_a}^{r}\rho r \ln\frac{r}{r_a} dr . \qquad (66)$$

Equation 66 is the required expression for the average potential at any radius in the charge region of the beam. If we substitute the power series expansion for ρ, (50), into this equation and perform the indicated integrations, we arrive at a rather unwieldy but general explicit form for $\bar{\varphi}$, from which we can easily extract the corresponding expressions for several special cases.

$$\bar{\varphi} = a \ln\frac{r}{r_1} + \varphi_1 - \frac{1}{\varepsilon}\sum_{n=0}^{\infty}\frac{\rho_n}{(n+2)^2}(r^{n+2} - r_a^{n+2})$$

$$+ \frac{1}{\varepsilon}\sum_{n=0}^{\infty}\frac{\rho_n}{n+2} r_a^{n+2}\ln\frac{r}{r_a} . \qquad (67)$$

Evaluation of α and γ

The potential $\bar{\varphi}$ expressed in the above equations applies to a uniform beam in which there is no radial motion. The potential φ as experienced by an electron and as used in sec. II applies when there is a radial motion in the beam provided electron shells do not cross each other. When the amplitude of radial oscillation is zero, or when the beam is in its equilibrium condition both $\bar{\varphi}$ and φ must agree, and moreover the radial electric fields derivable from $\bar{\varphi}$ and φ must agree. Since $\varphi = \alpha \ln r/r_o + \gamma$, then at $r = r_o$ where $\varphi = \bar{\varphi}$

$$\gamma = [\varphi]_{r=r_o} = [\bar{\varphi}]_{r=r_o} . \tag{68}$$

The more explicit forms of (68) are as follows

$$\gamma = a \ln \frac{r_o}{r_1} + \varphi_1 - \frac{1}{\varepsilon} \ln \frac{r_o}{r_a} \int_{r_a}^{r_o} \rho r dr + \frac{1}{\varepsilon} \int_{r_a}^{r_o} \rho r \ln \frac{r}{r_a} dr \tag{69}$$

and

$$\gamma = a \ln \frac{r_o}{r_1} + \varphi_1 - \frac{1}{\varepsilon} \sum_{n=0}^{\infty} \frac{\rho_n}{(n+2)^2} (r_o^{n+2} - r_a^{n+2})$$

$$+ \frac{1}{\varepsilon} \sum_{n=0}^{\infty} \frac{\rho_n}{n+2} r_a^{n+2} \ln \frac{r_o}{r_a} . \tag{70}$$

The condition on the radial electric fields at r_o states that

$$\left[\frac{\alpha}{r}\right]_{r=r_o} = \left[\frac{\partial \bar{\varphi}}{\partial r}\right]_{r=r_o} . \tag{71}$$

More explicitly, Eq. 71 becomes

$$\alpha = a - \frac{1}{\varepsilon} \int_{r_a}^{r_o} \rho r dr \tag{72}$$

and

$$\alpha = a - \frac{1}{\varepsilon} \sum_{n=0}^{\infty} \frac{\rho_n}{n+2} (r_o^{n+2} - r_a^{n+2}) . \tag{73}$$

The second term on the right of (72) represents the charge per unit length in the beam between radii r_a and r_o. Denoting this charge by q_o we may write

$$\alpha = a - \frac{q_o}{2\pi\varepsilon} \tag{74}$$

from which it is seen directly that α is a function of r_o which reduces to a when $r_o = r_a$. The value of α increases with r_o moreover, since q_o is necessarily negative in an electron beam, though α itself may be either positive

or negative. An equation that will be of considerable use in our design procedures is derived from (72).

$$\rho(r_o) = -\frac{\varepsilon}{r_o}\frac{\partial \alpha}{\partial r_o}. \tag{75}$$

In the last section it was indicated that the solution obtained is consistent with the assumption of noncrossing only if β is a constant, and this requires α to be proportional to r_o^2. Equation 75 shows that this is possible only if the charge density is uniform, i.e. independent of r_o. Although the uniform charge density is a necessary condition for consistency, it is not sufficient. Integration of (75) allows the addition of a constant, which, if it is not zero, does not allow α to be proportional to r_o^2. This constant is embodied in a and in the lower limit of integration in Eq. 72. In the case of a solid beam it is zero and the frequency β is constant, but for hollow beams, very special conditions are required to bring about the appropriate a, as might be imagined from the definition of a in Eqs. 64 and 65. In a later section this will be one of several special cases considered in detail.

With this background we shall proceed to a discussion of design procedures for this part of the beam system.

IV. A GENERAL METHOD FOR THE DESIGN OF THE INFINITE BEAM

This section is concerned with the methods of designing beam systems of the type discussed previously. The same restrictions apply here as elsewhere, and we treat only the longitudinally uniform section of the system without regard to the end conditions.

The design equations are nothing more than rearrangements of some of those appearing in the preceding two sections. To arrive at the most useful forms, we should consider our objective. Ordinarily the quantities predetermined by other considerations are the beam velocity, beam current and beam dimensions. Usually some of the following are also specified while the others must be chosen properly: radial charge or current distribution, electrode voltages, electrode geometry, and magnetic field configuration (cathode flux condition). The intensity of the magnetic field is usually a controllable quantity while its geometry may or may not be fixed by the particular application.

In choosing the quantities at our disposal, our object is to satisfy the equilibrium conditions of the beam, thereby minimizing the radial oscillation. We want to produce a longitudinally uniform beam, like that shown in Fig. 6, in which all electrons travel on constant radius paths with a common axial velocity.

The end conditions of such a beam are of vital importance in its attainment. Not only the cathode flux condition, but other restrictions have to be satisfied in the cathode region and any other places where the magnetic field is not axial and uniform. While the parameter adjustments to be discussed in this section are not sufficient to guarantee equilibrium, they are necessary. The end conditions that must also be satisfied are considered separately in the next section. Here we shall assume that these end conditions are appropriate and that the cathode flux condition is satisfied.

To find the equilibrium state, we return to the results of sec. II. From (42) we see that the amplitude of oscillation is zero if

$$x^2 = 0 \ . \tag{76}$$

But

$$x^2 = 2(b_o/R_o - 1)$$

or

$$x^2 = \frac{-2K(\gamma - V) - (\sqrt{1 + K\alpha} - 1)^2}{2 + K\alpha} \ . \tag{77}$$

Setting $x^2 = 0$ and solving for the optimum value of $\gamma - V$ gives us

$$(\gamma - V)_{opt.} = \frac{(\sqrt{1 + K\alpha} - 1)^2}{-2K} \ . \tag{78}$$

There is no danger that the denominator in (77) will be zero as the real character of ψ_c guarantees that $K\alpha$ is always greater than -1, as was pointed out in the discussion of stability.

Equation 78 is the necessary equilibrium condition. It could have been derived directly from the differential Eq. 22 by setting $r = r_o$ and $\dot{r} = 0$ and then applying the cathode flux condition (27). This emphasizes that (78) already embodies the assumption that (27) is satisfied. As we expect, $(\gamma - V)_{opt.}$ is a positive quantity.

This equation has a geometrical interpretation that allows a relatively easy visualization of the design process. It may be represented by a single surface. A plaster model of this surface is shown in Fig. 7. The height represents the value of $(\gamma - V)_{opt.}$ on a linear scale, and the other two coordinates represent α on a linear scale and -K on a logarithmic one. The reasons for using these particular scales will become apparent in the discussion that follows.

For any one electron shell to remain in equilibrium its corresponding values of K, α, and $\gamma - V$ must satisfy (78) or the point represented by these constants must lie in the surface. If the entire beam is to remain in equilibrium, every representative point has to lie in the surface.

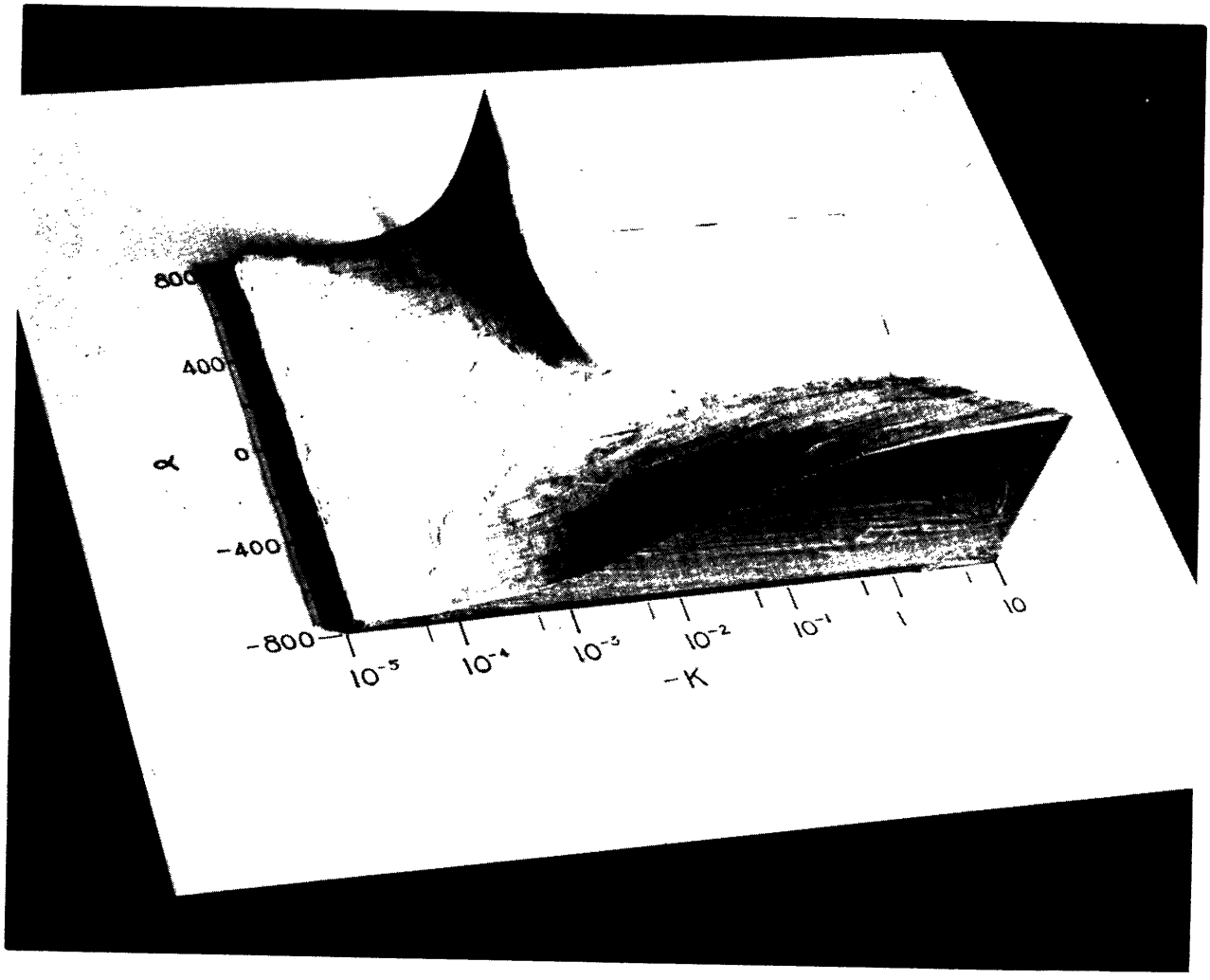

Fig. 7. Model of surface defined by Eq. 78.

Now consider any two shells in the beam, say the inside and outside edges. Reference to Eq. 71 shows that for the inside edge

$$\alpha_a = a \tag{79}$$

and for the outside edge

$$\alpha_b = a - \frac{Q}{2\pi\varepsilon} . \tag{80}$$

The difference between these two values of α is

$$\alpha_b - \alpha_a = - \frac{Q}{2\pi\varepsilon} \tag{81}$$

and depends on the total charge per unit length between the two shells. It is therefore fixed by the beam parameters alone. This constant difference is always a positive quantity for electron beams and is not affected by the actual values of the α's.

A similar statement may be made about the γ's for the two shells in question. For the inner edge

$$\gamma_a = a \ln \frac{r_a}{r_1} + \varphi_1 \tag{82}$$

from Eq. 69. Similarly, if we use the power series expansion for the charge density

$$\gamma_b = a \ln \frac{r_b}{r_1} + \varphi_1 - \frac{1}{\varepsilon} \sum_{n=0}^{\infty} \frac{\rho_n}{(n+2)^2} \left(r_b^{n+2} - r_a^{n+2} \right)$$

$$+ \frac{1}{\varepsilon} \sum_{n=0}^{\infty} \frac{\rho_n}{n+2} r_a^{n+2} \ln \frac{r_b}{r_a} . \tag{83}$$

The difference between these values is

$$\gamma_b - \gamma_a = \left(a + \frac{1}{\varepsilon} \sum_{n=0}^{\infty} \frac{\rho_n}{n+2} r_a^{n+2} \right) \ln \frac{r_b}{r_a}$$

$$- \frac{1}{\varepsilon} \sum_{n=0}^{\infty} \frac{\rho_n}{(n+2)^2} \left(r_b^{n+2} - r_a^{n+2} \right) \tag{84}$$

which is also unaffected by the particular value of either of the γ's. This difference is not solely dependent on the beam parameters, however, as the constant a involves the dimensions of the electrodes as well as those of the beam itself. Once the beam and electrode geometries are chosen, the difference expressed in (84) is specified. From the definition of K

$$K = \frac{e/m}{\omega_H^2 r_o^2}$$

it is apparent that the ratio of the two values of -K is a constant set by the beam geometry alone

$$\frac{-K_a}{-K_b} = \frac{r_b^2}{r_a^2} \tag{85}$$

as ω_H is the same for both shells. The difference between the logarithms of the -K's is thus a constant.

When these three differences, expressed in (81), (84), and the last statement, are taken together and interpreted geometrically in the same sense that defined the surface of Fig. 7, they define a rectangular prism or block of dimensions fixed by the beam parameters and the geometry of the system. The representative points for the inner and outer edges of the beam lie at opposite ends of a diagonal of this prism as illustrated in Fig. 8. The design procedure is now clear. It consists of moving the prism about in the coordinate space until the end points of the diagonal lie in the surface

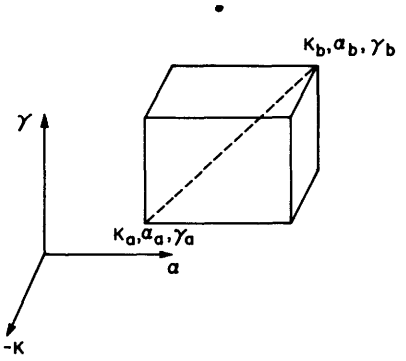

Fig. 8 The prism used in the design.

simultaneously. The final position is then used to calculate the potentials and the magnetic field.

While we have used two particular shells, the inside and outside ones, in the above development, any pair could have been chosen as examples. The procedure is thus perfectly general. The detailed behavior of the beam for any particular design condition may be obtained by repeated examination of the positions of the diagonal end points for various shells.

Before continuing this discussion, we reduce the method outlined above to something more practical by projecting the surface onto a plane and representing it as a family of curves. One possible projection is shown in Figs. 9 and 10 where α is chosen as parameter. The

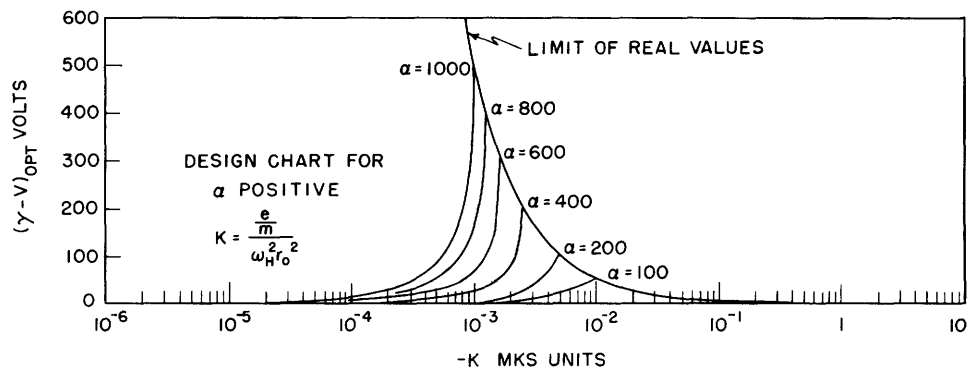

Fig. 9 Equation 78 with α positive.

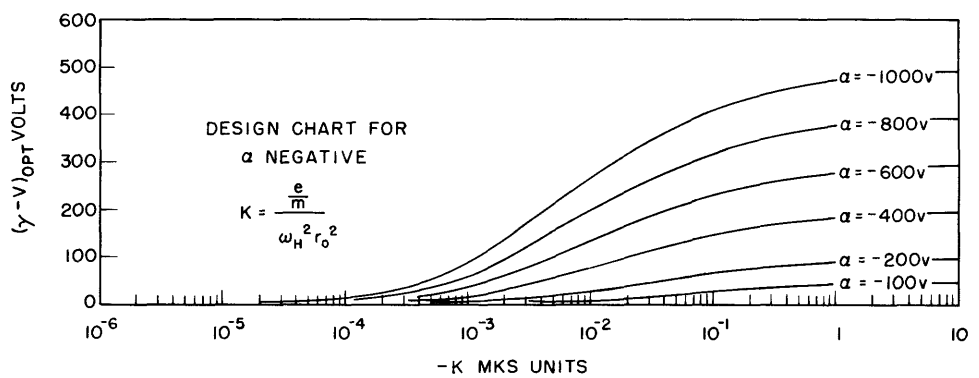

Fig. 10 Equation 78 with α negative.

projection of the design prism is a rectangle which is moved around on the design chart (Figs. 9 and 10) until the appropriate corners fall on two constant α curves which differ by the proper amount. As before, the resulting values of α, -K, and γ - V may be read for either of the corners and the

corresponding voltages and magnetic field determined from these.

In some cases it may happen that we do not have complete freedom in placing the rectangle where it will fit exactly as required. When this occurs, we must be careful to choose a position such that any error in $\gamma - V$ is an excess over the optimum value. If γ is smaller than the value needed to give zero oscillation at any particular radius, the electrons in that shell do not have enough energy to have the prescribed values of $\dot{z}$ and $r\dot{\theta}$. As the angular velocity is fixed by the magnetic field, the axial velocity will be too low, or the electrons will never get to the point in question. Figure 11 shows the correct method of placing the rectangle when it cannot be fitted to the curves ideally.

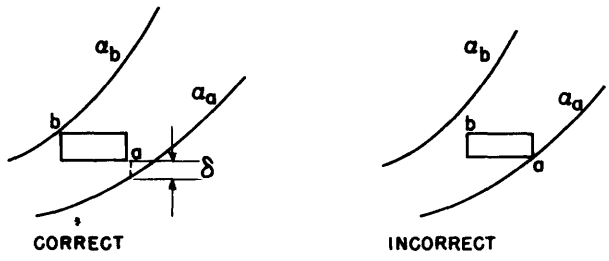

Fig. 11 Methods of placing the design rectangle on the chart.

If the rectangle is set so high that neither corner lies on the appropriate α curve, the entire beam must oscillate and our purpose of minimizing the oscillation is not achieved. In general then, we shall always set at least one corner of the rectangle on the appropriate curve. The question of which α curve is the appropriate one is settled by the choice of the end of the diagonal used to read off the final parameter values. Thus for any particular setting the parameters are read from the end that will make the other point err by an excess in γ. For example, on the right side of Fig. 11, instead of reading the parameter values from the point a as indicated, they should be read from the point b. Then the curve corresponding to the value of α at r_a will lie below a, as shown on the left.

This mention of errors in the design procedure leads us to consider their evaluation. This is obtained quite simply from the design chart. If the error in $\gamma - V$ is denoted by δ, as indicated in Fig. 11, then the actual value of $\gamma - V$ is given by

$$\gamma - V = (\gamma - V)_{opt.} + \delta \ . \tag{86}$$

Substituting (86) into (77) we obtain

$$x^2 = \frac{-2K(\gamma - V)_{opt.} - \left(\sqrt{1 + K\alpha} - 1\right)^2}{2 + K\alpha} - \frac{2K\delta}{2 + K\alpha} \ . \tag{87}$$

The first term of (87) is zero by definition of $(\gamma - V)_{opt.}$ and we are left with

$$x^2 = \frac{-2K\delta}{2 + K\alpha} \tag{88}$$

from which we can easily obtain the maximum and minimum limits of oscillation

by means of Fig. 4 or Eq. 42.

Once a location for the rectangle on the design chart is chosen we are left with the evaluation of the actual voltages to be applied to the electrodes and the magnetic field to be used; i.e. with the evaluation of φ_1, φ_2 and B.

The magnetic field is given directly by the chosen value of K. It is more convenient to use the representative point for the inside edge of the beam than any other. By definition

$$K_a = \frac{e/m}{\omega_H^2 r_a^2}$$

and

$$\omega_H = \frac{e}{m} \frac{B}{2} .$$

Therefore

$$B = \frac{2}{r_a \sqrt{e/m\ K}} . \tag{89}$$

The potentials are calculated from the equations developed in sec. III. At $r = r_a$ the integrals in (66) become zero and we have

$$\bar{\varphi}_a = \gamma_a = a \ln \frac{r_a}{r_1} + \varphi_1 \tag{90}$$

and

$$\varphi_1 = \gamma_a - a \ln \frac{r_a}{r_1} . \tag{91}$$

The value of a is given by Eq. 79

$$a = \alpha_a$$

Consequently

$$\varphi_1 = \gamma_a - \alpha_a \ln \frac{r_a}{r_1} \tag{92}$$

and

$$\varphi_2 - \varphi_1 = \alpha_a \ln \frac{r_2}{r_1} - \left[\frac{Q}{2\pi\varepsilon} \ln \frac{r_2}{r_b} + \frac{1}{\varepsilon} \sum_{n=0}^{\infty} \frac{\rho_n}{(n+2)^2} \left(r_b^{n+2} - r_a^{n+2} \right) \right.$$

$$\left. - \frac{1}{\varepsilon} \sum_{n=0}^{\infty} \frac{\rho_n}{n+2} r_a^{n+2} \ln \frac{r_b}{r_a} \right] . \tag{93}$$

Equations (89), (92), and (93) are used after the parameters α_a, γ_a, and K_a are chosen from the design chart.

The procedure outlined in this section is general in that it may be applied to a beam with an arbitrary radial charge distribution and no restriction has been placed on the problem other than those enumerated earlier. The design

chart is somewhat unwieldy because of this general character. In many cases the shape of the magnetic field in and near the cathode region is limited to certain special configurations. These limitations control the possible charge distributions in the beam. It is this practical restriction imposed by the magnetic field which narrows our field of inquiry to a few special cases where the design procedure can be carried out without the use of the chart. Instead, Eq. 78 is used directly to find the proper values of α_a, γ_a, and K_a, and then (89), (92), and (93) are applied to complete the design of this section of the beam system.

The next section, in which we examine the end conditions shows how these special cases arise.

V. END CONDITIONS: INJECTION OF THE BEAM

Up to this point we have considered only one part of the problem of producing electron beams in a magnetic focusing field. We have learned how a beam, once in a uniform magnetic field, will behave, and what voltages and magnetic field strength are necessary for equilibrium. This behavior that has been analyzed is only one particular type or "mode" out of many possible ones. It is certainly possible, for example, to have a beam in equilibrium in which the axial velocity differs from shell to shell. In this section we take up the problem of finding means to bring about the particular type of operation that we want.

It is necessary to consider the following questions: How do we get the required current into the beam? How do we insure that all electrons will have the same axial velocity? How do we get the beam into the desired region (between r_a and r_b) so that it will stay there according to the analysis?

The answers to these questions proposed in this section are not intended to be general. Only one particular method of solving these problems is suggested, and it is to be emphasized that there are other and possibly more fruitful lines of attack which could have been followed. The particular viewpoint taken here was chosen because of relative simplicity.

The foregoing remarks should be borne in mind as they are the basis for many of the restrictions and assumptions to follow. The results of the limited analysis presented here will appear to be overly restrictive, but they are sufficiently flexible to allow for the discussion of a number of special cases to be presented in the next section.

The functions of the end region of the beam system are such that it is expedient to break it up into two distinct sections, the electron gun and the transition region. Each of these parts will be considered separately and the

functions of each will make the reason for the division evident.

The Electron Gun

The electron gun has its main use in supplying and controlling the beam current. It is not necessarily a function of the gun to accelerate the beam to the proper axial velocity or to any other particular velocity, but we shall assign this function to it. There are other requirements on the electron gun, imposed by the ultimate uses of these systems, specifically their application in microwave tubes.

In microwave tubes, as in most other devices, it is desirable to reduce the noise to a minimum. This is one of the principal reasons for this entire study, since an efficient transmission of the beam through the drift tubes means a small contribution to the tube noise from partition of the beam current. The beam itself should be relatively free of noise fluctuations produced by either shot effect or partition. To reduce the shot noise due to initial velocities of emission, the cathode must operate in the space-charge limited regime, and to reduce partition noise, interception of the beam by electrodes should be small. The Pierce type of electron gun satisfies both of these demands as it has a high transmission efficiency and is space-charge limited. It is the only kind of electron gun capable of supplying the high current densities required in these systems.

The Pierce gun is well described in the literature and needs no further comment here (refs. 14 and 15). Design procedures for Pierce guns are available only for certain cases in which the electron flow inside the gun itself is rectilinear. The design, moreover, does not include the effects of magnetic fields so that if we are to use available methods of gun design, we shall have to nullify the effect of the magnetic field.

It might be argued that if the magnetic field is to have no effect at the gun, then there should be no magnetic field, but this is not generally possible. If focusing is to be obtained, electrons must cross magnetic field lines and thereby acquire an angular velocity. Except for one special case, ψ_c must be some nonzero quantity, and it is always different from the flux ψ linked by the electron shell in the uniform part of the beam.

Of course, we can still retain a finite value of ψ_c and have no magnetic field in the gun region if we shield it. This procedure prevents magnetic flux from affecting the electron flow in the gun by guiding part of it through a central pole piece linking the cathode, and the remainder outside of the cathode as shown in Fig. 12.

In this configuration ψ_c is the same for all electrons regardless of the

position from which they originated at the cathode. The electron gun associated with such pole pieces operates independently of the magnetic field if the shielding is good enough.

Another way of nullifying the effect of the magnetic field in the gun is to have it parallel to the lines of electron flow that would exist even without the field. If this condition is obtained the field cannot affect the beam since ψ and ψ_c are the same for any individual electron so long as it remains in the gun. The angular velocity is zero and the conditions assumed in designing the gun hold true.

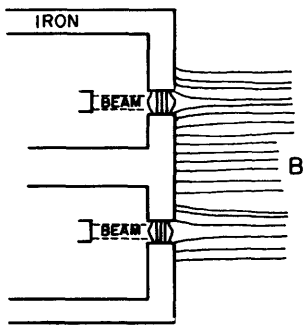

Fig. 12 A magnetically shielded electron gun.

This alternative configuration insures that the magnetic field in the immediate vicinity of the cathode is normal to it. The significance of the fact is considerably greater than that it allows us to design the gun. It means that we can be reasonably sure that thermal velocities of emission have negligible influence on the problem and that the noise will not be excessive.

Suppose there were a magnetic field oblique to the cathode surface in its immediate vicinity. The component of field parallel to the cathode surface where the electron velocities are low bends the trajectories around and builds up a high space-charge density which suppresses any further emission. This situation is analogous to that in the cut-off magnetron. In order to get a true picture of the potential and space-charge distribution in this case, we should have to take into account the thermal velocities of emission. Twiss (ref. 16) has considered this problem and has shown that neglect of thermal velocities in these cases can lead to serious error. Where the field is parallel to the electron paths and normal to the cathode, the Pierce gun should operate almost as though there were no magnetic field, and experience has shown that in this case thermal velocities introduce little error. Twiss has also shown that a large part of the preoscillation noise in the magnetron arises from the situation just discussed. The relative motions of the various streams of electrons moving out from the cathode and back towards it produces space-charge amplification of the noise already present. This mechanism is absent to a large extent in the system proposed here where the magnetic field is purely normal to the cathode surface.

It was mentioned earlier that we would assign to the gun the function of accelerating the beam to some particular voltage. The main reason for this is to get the electrons to a high enough velocity before they start to cross field lines. If this is not true, we get into the same trouble as we would

if we had the transverse field near the cathode. With a previous acceleration the effect of the transverse field is, to a high degree of accuracy, the same for all electrons, having a common ψ_c so that we can be quite sure there is no serious error due to the thermal velocity distribution.

The Transition Region

The role of the transition region should now be apparent. It is in this part of the system that the beam crosses magnetic field lines and acquires the angular velocity it needs for focusing in the useful part of the system. The electron trajectories at the two extremes of this region are specified; at the gun anode all electrons have essentially the same axial velocity, and at the beginning of the uniform field, all electrons must have a common specified axial velocity, the proper angular velocity and no radial velocity. Our problem now is to find a trajectory in the transition region that links the gun and the uniform field sections and has the properties just mentioned at either of its ends.

It is not possible to solve for this trajectory unless the geometry and potentials of the system are entirely specified, but it is our object to find the geometry and required potentials in the transition space. Finding the electron path from a set of known conditions where the magnetic field is non-uniform is an extremely difficult task. It would involve a repetition of the analysis of sec. II where the z independence is lost. The alternative is to specify a trajectory with the necessary characteristics and then to find the geometry and potentials consistent with the assumed electron motion.

The simplest path we can assume is a constant radius one. This results in a system having the general form of that shown in Fig. 13 where the electron beam maintains its shape all the way from the anode of the gun through the uniform part of the system where it is put to use. The constant radius path clearly satisfies the conditions necessary at the gun anode and at the entrance to the drift tubes. The problem to be solved now is to find the conditions which correspond to the assumed path and how to satisfy these conditions by shaping the electrodes as indicated in Fig. 13.

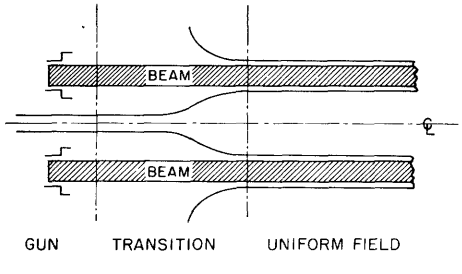

Fig. 13 Constant radius beam system.

The magnetic field configuration is assumed to be known everywhere, so we have to find the electric potentials and fields that, in combination with the magnetic field, will keep the electrons on their specified paths. We

return to the Lagrangian used in sec. II.

$$L = -e\varphi + eA_\theta r\dot{\theta} + \frac{m}{2}\left(\dot{r}^2 + r^2\dot{\theta}^2 + \dot{z}^2\right) . \tag{94}$$

The equations of motion are derived from Euler's equation

$$\frac{d}{dt}\left(\frac{\partial L}{\partial \dot{q}_i}\right) - \frac{\partial L}{\partial q_i} = 0 . \tag{95}$$

Substitution of (94) into (95) for the θ component gave us Busch's theorem

$$\dot{\theta} = \frac{e}{mr^2}\left(A_c r_c - A_\theta r\right) . \tag{96}$$

By symmetry

$$\frac{\partial \varphi}{\partial \theta} = 0 . \tag{97}$$

If the trajectories are to have a constant radius, the radial force must be zero. A relation between the radial electric field and the magnetic field is determined. The radial force is given by $-\partial L/\partial r$.

$$\frac{\partial L}{\partial r} = 0 = -e\frac{\partial \varphi}{\partial r} + eA_\theta\dot{\theta} + er\dot{\theta}\frac{\partial A_\theta}{\partial r} + mr\dot{\theta}^2 . \tag{98}$$

Consequently

$$\frac{\partial \varphi}{\partial r} = A_\theta\dot{\theta} + r\dot{\theta}\frac{\partial A_\theta}{\partial r} + \frac{m}{e}r\dot{\theta}^2 . \tag{99}$$

The angular velocity is eliminated from the last equation by means of Eq. 96.

$$\frac{\partial \varphi}{\partial r} = \frac{e}{mr^2}\left(r_c A_c - rA_\theta\right)\left(r\frac{\partial A_\theta}{\partial r} + r_c\frac{A_c}{r}\right) . \tag{100}$$

This equation can be simplified by means of an assumption about the magnetic field. It is a rather good approximation, as shown in an appendix, that for a system using solenoids but no iron, the flux is proportional to r^2 at any cross-section. The axial component of flux density B_z is therefore a function of z alone . Because

$$\psi = 2\pi rA_\theta = \pi r^2 B_z \tag{101}$$

it is easily shown that

$$\frac{A_\theta}{r} = \frac{\partial A_\theta}{\partial r} . \tag{102}$$

With this approximation (100) becomes

$$\frac{\partial \varphi}{\partial r} = -\frac{e}{mr^3}\left[(rA_\theta)^2 - (r_c A_c)^2\right] \tag{103}$$

and this is put in the more understandable form

$$\frac{\partial \varphi}{\partial r} = -\frac{e}{m}\frac{1}{4\pi^2 r^3}\left(\psi^2 - \psi_c{}^2\right) . \tag{104}$$

Note that Eq. 104 reduces to zero inside the electron gun where ψ and ψ_c

are equal, and to the equilibrium conditions already derived when ψ is $\pi r_o^2 B$ and ψ_c is specified by the cathode flux condition. This relationship between the radial electric field and the magnetic field is the only specification that must be met in the transition region. In satisfying it, the potential φ along the beam will take up certain values according to Laplace's and Poisson's equation. It is interesting to examine the effects of this potential variation.

As the radial velocity is zero and the angular velocity is controlled completely by the magnetic field, variations in potential can affect only the axial velocity. The energy equation (1) becomes

$$\dot{z}^2 = -2\frac{e}{m}\varphi - r^2\dot{\theta}^2 \tag{105}$$

and with the use of Busch's theorem we obtain

$$\dot{z}^2 = -2\frac{e}{m}\varphi - \frac{(e/m)^2}{4\pi^2 r^2}(\psi_c - \psi)^2 . \tag{106}$$

At the anode of the electron gun the second term on the right is absent and the potential must be the anode potential. In the uniform field section the potential is specified by the magnetic field and the required angular velocity and must be higher than the gun anode potential to account for the rotational energy. Between these places the potential is relatively free to take up any value but we should be careful about one thing. If the potential becomes too low, it is possible for the axial velocity to become zero. Electrons are then reflected instead of passing through the transition region. Even if the axial velocity does not go to zero but reaches a very low value at some point, the thermal velocities will again come into play and there is a possibility of increased noise. In general, however, the potential along the beam will be a smoothly varying function as the magnetic field itself is.

So far, the relatively easy task of finding the conditions necessary in the transition region has been carried out. The task of learning how to establish these conditions in practice is a much more difficult one. An exhaustive study of this problem would be a major undertaking and is beyond the scope of this paper. The remainder of this section is devoted to pointing out some of the difficulties involved and to a suggested method of design. The method is outlined only and is not presented in full detail as it is not completely rigorous. It is offered here as a possible start on the practical solution of the problem.

The design method which suggests itself is the use of the electrolytic tank in a manner paralleling that of the Pierce gun design. The space-charge and boundary conditions involved in the transition region complicate the picture so that the tank cannot be used directly.

In the design of the Pierce gun, the boundary condition along the edge of the

beam is that there be no normal electric field. This condition can be simulated in the tank by a strip of dielectric and then attention need be paid only to the region outside the beam where Laplace's equation applies, as it does in the tank. The transition region requires an electric gradient at the edge of the beam so that the entire system must be included in a tank design. The only way to include the effects of space charge in the electrolytic tank (ref. 17) is a difficult and indirect one.

To avoid these difficulties we make one further restriction, that the axial velocity be constant and correspond to the voltage V all through the transition region. This restriction fixes the charge density and the beam appears perfectly uniform all along its length, except for an increase in the angular velocity along the axis. With this uniform beam it is easy to calculate the radial potential gradient due to space-charge only.

For the case where we have air-core coils and the cathode is in a uniform magnetic field, the radial potential gradient demanded by the dynamics of the transition region is given in Eq. 104

$$\frac{\partial \varphi}{\partial r} = -\frac{e}{m}\frac{1}{4\pi^2 r^3}\left(\psi^2 - \psi_c{}^2\right) .$$

The potential gradient due to space-charge in the beam is given by

$$\frac{\partial \varphi_s}{\partial r} = -\frac{1}{2\pi\varepsilon r}\int_{r_a}^{r} \rho r dr \qquad (107)$$

where the notation used in sec. III is adopted here. It will be shown in the next section that with the magnetic field configuration assumed here the charge density is uniform. Then (107) becomes

$$\frac{\partial \varphi_s}{\partial r} = -\frac{\rho_o}{4\pi\varepsilon}\left(r - \frac{r_a{}^2}{r}\right). \qquad (108)$$

The total gradient $\partial\varphi/\partial r$ must be made up of that due to space charge and that due to the electrodes. The gradient due to the electrodes is therefore

$$\frac{\partial \varphi_L}{\partial r} = \frac{\partial \varphi}{\partial r} - \frac{\partial \varphi_s}{\partial r} \qquad (109)$$

where φ_L is a solution to Laplace's equation. Substituting (104), (108), and (101) into (109) we obtain

$$\frac{\partial \varphi_L}{\partial r} = -\frac{e}{m}\frac{r}{4}\left(B_z{}^2 - B_c{}^2\right) + \frac{\rho_o}{4\pi\varepsilon}\left(r - \frac{r_a{}^2}{r}\right) . \qquad (110)$$

This is the condition that must be satisfied by the electrodes. In the next section it is shown that in the uniform beam region, B, the final value of B_z is so chosen that the terms in r cancel and we are left with a gradient inversely proportional to r. This gradient is satisfied by the proper voltage difference between the inner and outer electrodes. It is a job for the

electrolytic tank to determine the shapes of electrodes required to produce the field specified in (110). This can be done by means of pairs of probes set in the tank. The potential difference across these pairs is a measure of the field along the line joining them. At first sight it may appear that the problem is solved but there are several difficulties which should be noted. First is the question of whether it is possible by means of electrodes, preferably only two, to set up a field with the functional form expressed in (110). It is possible in the uniform section, but perhaps only approximately so in the transition.

The second difficulty is that we do not know what potential to apply to the outer electrode in the tank. Its actual potential, as pointed out in sec. III, has a contribution due to space charge. The potential to be used in the tank must not include this component. But we do not know what the space-charge component is because it depends on the radius of the electrode, and that is what we are trying to find. A possible way out of this dilemma is to use any shape electrode and potential in the tank that will satisfy (110). When the tube is built with this shape of electrode, its potential can be adjusted until satisfactory results are obtained.

The third difficulty will be more readily appreciated after this case is considered in the next section. It is shown there that even though the radial forces can be balanced in the uniform section, as just mentioned, the potential variation with radius is not the optimum one and some oscillation of the beam must occur. It is possible to fix the equilibrium position of each shell but it is not possible to make each shell stay at its equilibrium position; rather it oscillates about this radius. We should expect a similar situation to occur in the transition region, as it blends into the uniform section. We may expect therefore that it will not be possible to keep the beam entirely in equilibrium through the transition region.

The above remarks are intended principally to show the nature of the problem of the transition region, even in the very restricted case chosen here. It is clearly a difficult problem and its solution requires a careful and painstaking analysis. The benefits of such an analysis would, in the opinion of the author, be far greater than those coming from the solution of this particular case. The understanding to be gained and the method of solution should be extremely useful in a great variety of cases, particularly with the increasing use of electron beams.

Another method of solving this problem, and one that perhaps would yield more immediate results for this special case, is the experimental approach. A few electrodes both inside and outside the beam, with adjustable potentials applied to them may very well provide sufficient flexibility to enable the

beam to come through the transition region. This approach, by yielding some observable results, may also add enough insight to give impetus to a theoretical analysis. Some hope for its success is given by the results of an experiment to be described in sec. VIII.

VI. SPECIAL CASES

Having considered the general theory, design methods, and conditions in the cathode and transition regions, we turn now to a discussion of some cases of practical interest. Explicit design formulae are developed in this section for those cases which are most likely to arise in actual practice. The results given here, therefore, are directly useful in design work and are given in a form suited to that purpose.

In the last section it was shown that the magnetic field had to be absent from the cathode region or normal to the surface of the cathode. The two broad categories into which the cases to be discussed fall are based on this division. In one group of cases the magnetic field at the cathode is taken as uniform of value B_c different from that in the beam. In the other group it is assumed that the gun is magnetically shielded and the flux ψ_c linking the cathode circle is the same for all electrons in the beam. Each of these main divisions is further subdivided into the several cases chosen because of various practical reasons.

We consider first the group of cases in which the magnetic field at the cathode is uniform.

Division I $\psi_c = \pi r_o^2 B_c$

In addition to specifying that the field at the cathode is uniform, we make the assumption that the flux linking the cathode circle for any electron shell of equilibrium radius r_o can be expressed by

$$\psi_c = \pi r_o^2 B_c \ . \tag{111}$$

This is certainly true when the beam retains its diameter from the cathode all the way through the uniform beam section as indicated in Fig. 12. Here B_c is the actual flux density in the gun region. Equation 111 may be true, however, in other cases where the beam does not remain uniform and then B_c represents an effective flux density at the cathode.

Substituting (111) into (27) and squaring we obtain

$$1 + K\alpha = \left(\frac{B_c}{B}\right)^2 . \tag{112}$$

Solving for α and using the definition of K, (26), we see that

$$\alpha = \frac{e}{m}\frac{r_o^2}{4}\left(B_c^2 - B^2\right) \tag{113}$$

and from (75)

$$\rho = -\frac{\varepsilon}{r_o}\frac{\partial\alpha}{\partial r_o} = -\frac{e}{m}\frac{\varepsilon}{2}\left(B_c^2 - B^2\right) . \tag{114}$$

The last three equations make it clear that in this case our assumption of noncrossing can be a valid one. Indeed, we have chosen $K\alpha$ as a constant independent of r_o in writing (112), and this ensures that the frequency of oscillation β is independent of r_o. If the electrons all have the same phase of radial oscillation and if their amplitudes are a continuous function of r_o then the assumption is true. This particular group, then, is of interest, as we can be reasonably sure that the analysis is consistent throughout.

As the charge density is uniform we can denote it by the constant term ρ_o in its power series expansion (50). It will be convenient to use the following notation also

$$B^2 - B_c^2 = B_{eff.}^2 \tag{115}$$

where $B_{eff.}$ denotes an effective value of magnetic field. The reason for this notation is that it enables us to write a single design equation for all the cases to follow, if $B_{eff.}$ is properly defined for each one.

Equation 114 becomes

$$\rho_o = \frac{e}{m}\frac{\varepsilon}{2}B_{eff.}^2 . \tag{116}$$

If we are to have an electron beam, ρ_o must be numerically negative and $B_{eff.}$ must be real, the flux density in the main part of the beam must therefore be greater than that in the gun. When these densities are equal, the allowable charge density is zero, because we cannot have magnetic focusing unless electrons cross magnetic field lines. For any chosen beam density $B_{eff.}$ is specified by (116) and the greatest economy of magnetic field is obtained when $B_c = 0$. Power is saved because the magnetic field at the cathode is eliminated, and also because the field strength in the rest of the system is a minimum.

To find the magnetic field strength required for any charge density we solve (116) for $B_{eff.}^2$

$$B_{eff.}^2 = \frac{2\rho_o}{\varepsilon\ e/m} . \tag{117}$$

The numerical value of ρ_o is obtained from the specified beam voltage V and current I. The density is given by

$$\rho_o = -J/\dot{z} \tag{118}$$

where J is the axial current density, and since it is uniform, it is just the total current divided by the area of the beam.

$$J = \frac{I}{\pi(r_b^2 - r_a^2)} . \tag{119}$$

These equations substituted into (117) with the value of $\dot{z}$ obtained from (17) give us the important design equation

$$B_{eff.}^2 = \frac{2}{\varepsilon\, e/m\, \pi \sqrt{-2\, e/m}(r_b^2 - r_a^2)} \frac{I}{\sqrt{V}} = \frac{6.9 \times 10^{-7}}{r_b^2 - r_a^2} \frac{I}{\sqrt{V}} \tag{120}$$

Before going on to find the electrode voltages to apply, we shall see whether it is possible to satisfy the Eq. 78 demanded by equilibrium conditions. To do this, we compare the actual value of $\gamma - V$ with the optimum value.

From Eq. 70, the actual value of $\gamma - V$ is given by

$$\gamma - V = a \ln \frac{r_o}{r_1} + (\varphi_1 - V) - \frac{\rho_o}{4\varepsilon}(r_o^2 - r_a^2) + \frac{\rho_o}{2\varepsilon} r_a^2 \ln \frac{r_o}{r_a} \tag{121}$$

but a is just the value of α at $r_o = r_a$. From (113) and (116)

$$a = -\frac{e}{m}\frac{r_a^2}{4} B_{eff.}^2 = -\frac{\rho_o r_a^2}{2\varepsilon} . \tag{122}$$

With the use of (122), Eq. 121 simplifies to

$$\gamma - V = a\left(\ln \frac{r_a}{r_1} - \frac{1}{2}\right) + (\varphi_1 - V) + \frac{a}{2}\frac{r_o^2}{r_a^2} . \tag{123}$$

The optimum value of $\gamma - V$ is obtained from (78)

$$(\gamma - V)_{opt.} = \frac{(\sqrt{1 + K\alpha} - 1)^2}{-2K}$$

which, on subsitution of (112), becomes

$$(\gamma - V)_{opt.} = -\frac{e}{m}\frac{r_o^2}{8}(B_c - B)^2 . \tag{124}$$

The difference between the actual and optimum values of $\gamma - V$, after simplification, is written

$$(\gamma - V) - (\gamma - V)_{opt.} = (\varphi_1 - V) - \frac{e}{m}\frac{r_a^2}{4}(B^2 - B_c^2)\left(\ln \frac{r_a}{r_1} - \frac{1}{2}\right) + \frac{e}{m}\frac{r_o^2}{4} B_c (B_c - B) . \tag{125}$$

The last term on the right is the only one depending on r_o and it is positive. The error expressed in (125) which is just δ defined in (86), is therefore an increasing function of r_o. It cannot be made zero for all values of r_o unless $B_c = 0$ or $B_c = B$. The latter possibility is of little interest as it demands zero charge density. The former will be considered shortly.

Since the error δ must be positive and cannot be zero generally, the beam must oscillate. The best we can do is to set $\delta = 0$ at $r_o = r_a$. When this is done, we obtain the design equation for the potential applied to the inner electrode.

$$\varphi_1 = V + \frac{e}{m}\frac{r_a^2}{4}\left[(B^2 - B_c^2)\left(\ln\frac{r_a}{r_1} - \frac{1}{2}\right) - (B_c^2 - BB_c)\right] . \qquad (126)$$

If we let

$$\sqrt{1 + K\alpha} = g_1 \qquad (127)$$

so that

$$B_c = Bg_1$$

then Eq. 126 is written

$$\varphi_1 = V + \frac{e}{m}\frac{r_a^2}{4} B^2\left[(1 - g_1^2)\ln\frac{r_a}{r_1} + \frac{3}{2}g_1^2 - g_1 - \frac{1}{2}\right] . \qquad (128)$$

The corresponding expression for the potential difference between inside and outside electrodes is derived from Eq. 93

$$\varphi_2 - \varphi_1 = -\frac{e}{m}\frac{r_a^2}{4} B_{eff.}^2\left[\left(\ln\frac{r_2\, r_a}{r_1\, r_b} - \frac{1}{2}\right) + \frac{r_b^2}{r_a^2}\left(\ln\frac{r_2}{r_b} + \frac{1}{2}\right)\right] . \qquad (129)$$

This potential difference is always positive as it must be in order to make α positive. It is necessary to supply an outward electric force in addition to that of the space charge to focus the beam. The magnetic field in this case spins electrons around the axis faster than necessary just to overcome their own repulsion forces. Even with $B_c = 0$ which is the most economical magnetic field configuration under this heading, we have too much field strength, the angular velocity is too great and we must aggravate the effects of space charge to balance the forces and obtain focusing.

In the general case when $B_c \neq 0$, the beam must oscillate everywhere except at the inner edge. The amplitude of oscillation increases with r_o and the error in potential is given by

$$\delta = -\frac{e}{m}\frac{B^2}{4} g_1(1 - g_1)(r_o^2 - r_a^2) \qquad (130)$$

when Eq. 128 is satisfied. Then, from (88)

$$x^2 = \frac{2g_1(1 - g_1)}{(1 + g_1^2)}\left(1 - \frac{r_a^2}{r_o^2}\right) . \qquad (131)$$

Zero Field at the Cathode $B_c = 0$

This special case of the preceding one is of interest because it is the only one in this division where the beam can be in equilibrium and because it leads us to the very important case of the uniform solid beam.

When $B_c = 0$, $g_1 = 0$ and the design equations from the previous section are simplified. From (115)

$$B_{eff.}^2 = B^2 . \qquad (132)$$

Equation 120 remains unchanged, (128) becomes

$$\varphi_1 = V + \frac{e}{m}\frac{r_a^2}{4} B^2 \left(\ln \frac{r_a}{r_1} - \frac{1}{2} \right) \tag{133}$$

and (129) remains unchanged. Equation 133 is of interest. The potential on the inner electrode is greater than V if $\ln r_a/r_1 < 1/2$. If the inner electrode becomes small enough, its potential can be less than V, and may even become negative. We can never let the inner electrode become an infinitesimal wire along the axis, as that would require an infinite negative voltage on it.

Solid Beam

When the beam is solid, we can forget the inner electrode, and we let $r_a = 0$. Because of symmetry, the radial electric field at the axis must be zero so a is zero. But α has the same form as a with r_o substituted for r_a. Hence

$$\alpha = - \frac{\rho_o r_a^2}{2\varepsilon} \tag{134}$$

from (122). Equation 121 simplifies to

$$\gamma - V = - \frac{\rho_o r_o^2}{4\varepsilon} \tag{135}$$

since $\gamma - V$ must be zero at the axis. A similar development to that carried out previously shows that B_c must be zero for the equilibrium condition to be satisfied. Equation 120 remains unchanged except that $r_a = 0$. The potential of the outer electrode may be derived by integration as was done in sec. III, or directly from (129). The result of this computation is

$$\varphi_2 = V - \frac{\rho_o r_b^2}{2\varepsilon} \left(\ln \frac{r_2}{r_b} + \frac{1}{2} \right) \tag{136}$$

which with (117) becomes

$$\varphi_2 = V - \frac{e}{m}\frac{B^2 r_b^2}{4} \left(\ln \frac{r_2}{r_b} + \frac{1}{2} \right). \tag{137}$$

There is no other category in which the solid beam may be put. We cannot specify that ψ_c be some nonzero value for all electrons as this requires a ring-shaped cathode with a magnetic pole-piece through it. Electrons starting off the axis can never approach arbitrarily close to it, as was shown in sec. II. The cathode supplying a solid beam must lie on and around the axis and so must be classed in this first group. The most efficient and economical operation is obtained when the magnetic field does not penetrate into the cathode region.

Division II Shielded Guns

In this division the analysis parallels that just given. The electron guns

are assumed to be built in such a manner that the inside region where electrons are first accelerated is completely shielded from the magnetic field. In this case the flux ψ_c linking the cathode circle is the same for every electron in the beam, regardless of the position on the cathode from which it started.

Solving (27) for α, when ψ_c is independent of r_o we get

$$\alpha = \frac{e/m}{4\pi^2 r_o^2} \left(\psi_c^2 - \pi^2 r_o^4 B^2\right) \tag{138}$$

and the charge density ρ is obtained from (75)

$$\rho = -\frac{\varepsilon}{r_o}\frac{\partial \alpha}{\partial r_o} = \frac{e}{m}\frac{\varepsilon}{2}\left(\frac{\psi_c^2}{\pi^2 r_o^4} + B^2\right) . \tag{139}$$

The sign of ρ depends only on the sign of the electron charge; no precautions need be taken to ensure that we get a finite charge density. This density is no longer uniform but has a term proportional to $1/r_o^4$ added to it. It is significant that the charge density is now increased over the value it would have if ψ_c were zero, whereas in the previous division the allowable charge density was decreased by any flux linking the cathode. It is this difference which enables us to focus a beam with no magnetic field in the uniform section, a special case to be treated soon.

The total charge per unit length Q is given by either of the following expressions

$$Q = \frac{I}{\sqrt{-2\ e/m\ V}} = \int_{r_a}^{r_b} 2\pi r_o \rho dr_o . \tag{140}$$

The integral is easily evaluated. It is, with (139) substituted for ρ

$$Q = \pi \frac{e}{m}\frac{\varepsilon}{2}\left(r_b^2 - r_a^2\right)\left(\frac{\psi_c^2}{\pi^2 r_a^2 r_b^2} + B^2\right) \tag{141}$$

and solving for the factor on the right we obtain

$$\left(\frac{\psi_c}{\pi r_a r_b}\right)^2 + B^2 = \frac{2}{e/m\ \varepsilon\pi\sqrt{-2\ e/m}\left(r_b^2 - r_a^2\right)}\frac{I}{\sqrt{V}} \tag{142}$$

which is identical to (120) if we define

$$B_{eff.}^2 = \left(\frac{\psi_c}{\pi r_a r_b}\right)^2 + B^2 . \tag{143}$$

We now compare the actual and optimum values of $\gamma - V$. The actual value of $\gamma - V$ may be written in terms of the two components of charge density ρ_o and ρ_{-4} where we extend the definition in (50) so that

$$\rho = \rho_o + \frac{\rho_{-4}}{r_o^4} . \tag{144}$$

Then, from (70)

$$\gamma - V = \left(a + \frac{\rho_o}{2\varepsilon} r_a^2 - \frac{\rho_{-4}}{2\varepsilon} \frac{1}{r_a^2} \right) \ln \frac{r_o}{r_a} + a \ln \frac{r_a}{r_1} + (\varphi_1 - V)$$

$$- \frac{\rho_o}{4\varepsilon} (r_o^2 - r_a^2) - \frac{\rho_{-4}}{4\varepsilon} \left(\frac{1}{r_o^2} - \frac{1}{r_a^2} \right) \tag{145}$$

and from (138) and (78)

$$(\gamma - V)_{opt.} = - \frac{e}{m} \left(\frac{\psi_c^2}{8\pi^2 r_o^2} + \frac{r_o^2 B^2}{8} - \frac{B\psi_c}{4\pi} \right). \tag{146}$$

By matching the coefficients of the various powers of r_o in both (145) and (146) we obtain the following set of equations

$$a + \frac{\rho_o r_a^2}{2\varepsilon} - \frac{\rho_{-4}}{2\varepsilon r_a^2} = 0 \tag{147}$$

$$a \ln \frac{r_a}{r_1} + (\varphi_1 - V) + \frac{\rho_o r_a^2}{4\varepsilon} + \frac{\rho_{-4}}{4\varepsilon r_a^2} = \frac{e}{m} \frac{B\psi_c}{4\pi} \tag{148}$$

$$- \frac{\rho_o}{4\varepsilon} = - \frac{e}{m} \frac{B^2}{8} \tag{149}$$

$$- \frac{\rho_{-4}}{4\varepsilon} = - \frac{e}{m} \frac{\psi_c^2}{8\pi^2} \quad . \tag{150}$$

Reference to Eq. 139 shows that both (149) and (150) are true, according to the definitions of ρ_o and ρ_{-4}. Solving (148) for φ_1 with the value of a obtained from (147) we obtain

$$\varphi_1 = V + \frac{e}{4m} \left[\ln \frac{r_a}{r_1} \left(B^2 r_a^2 - \frac{\psi_c^2}{\pi^2 r_a^2} \right) - \frac{1}{2} \left(\frac{\psi_c}{\pi r_a} - B r_a \right)^2 \right] \tag{151}$$

and we may use (65) or (93) to solve for the value of

$$\varphi_2 - \varphi_1 = \frac{e}{4m} \left[\frac{\psi_c^2}{\pi^2 r_a^2} \left(\ln \frac{r_a}{r_1} + \frac{1}{2} \right) + \frac{\psi_c^2}{\pi^2 r_b^2} \left(\ln \frac{r_2}{r_b} - \frac{1}{2} \right) \right.$$

$$\left. - B^2 r_a^2 \left(\ln \frac{r_a}{r_1} - \frac{1}{2} \right) - B^2 r_b^2 \left(\ln \frac{r_2}{r_b} + \frac{1}{2} \right) \right] . \tag{152}$$

It is thus possible to arrive at appropriate potentials and magnetic field values to keep the beam in equilibrium for the general case in which ψ_c is the same for all electrons.

The term $\psi_c/(\pi r_a r_b)$ which combined with B makes up the effective magnetic field, has the form of a geometric mean flux density at the cathode. This suggests making a substitution similar to that made in the previous section. We let

$$\frac{\psi_c}{\pi r_a r_b} = g_2 B \ . \tag{153}$$

With this substitution Eqs. 151 and 152 become

$$\varphi_1 = V + \frac{e}{m}\frac{B^2}{4} r_a^2 \left[\ln \frac{r_a}{r_1}\left(1 - \frac{r_b^2}{r_a^2} g_2^2\right) - \frac{1}{2}\left(g_2 \frac{r_b}{r_a} - 1\right)^2 \right] \tag{154}$$

and

$$\varphi_2 - \varphi_1 = \frac{e}{m}\frac{B^2 r_a^2}{4}\left[g_2^2 \frac{r_b^2}{r_a^2}\left(\ln \frac{r_a}{r_1} + \frac{1}{2}\right) + g_2^2\left(\ln \frac{r_2}{r_b} - \frac{1}{2}\right) - \left(\ln \frac{r_a}{r_1} - \frac{1}{2}\right) - \frac{r_b^2}{r_a^2}\left(\ln \frac{r_2}{r_b} + \frac{1}{2}\right)\right] . \tag{155}$$

With these results, it is a simple matter to derive the equations for the several special cases arising in this group.

Both Drift Tubes at Same Potential

In many structures it may be desirable to have the drift tubes at the same potential to avoid insulation problems in the construction of the tube. The radio-frequency requirements may demand that both tubes be part of the same wave guiding structure and d-c separation of them may involve a great deal of difficulty with r-f chokes and other devices. If a shielded electron gun is used, it is possible to keep the tubes at the same potential and maintain a hollow beam. Equation 155 shows that g_2 must be adjusted to make $\varphi_2 - \varphi_1 = 0$. The necessary value of g_2 is evident.

$$g_2 = \left[\frac{\left(\ln \frac{r_a}{r_1} - \frac{1}{2}\right) + \frac{r_b^2}{r_a^2}\left(\ln \frac{r_2}{r_b} + \frac{1}{2}\right)}{\frac{r_b^2}{r_a^2}\left(\ln \frac{r_a}{r_1} + \frac{1}{2}\right) + \left(\ln \frac{r_2}{r_b} - \frac{1}{2}\right)} \right]^{\frac{1}{2}} \tag{156}$$

This value of g_2 which depends only on the geometry of the system then determines the necessary magnetic field strength and electrode voltage.

Inner Drift Tube Absent

This is another circumstance that may be dictated by the r-f properties of the tube. An obvious example is the helix type traveling-wave tube or a klystron-drift tube in which a hollow beam is used to increase the efficiency.

When there is no inner electrode, there can be no electric field inside the beam or at its inside edge. The constant a must therefore be zero. Equations 138 or 147 may be used to evaluate a and the result is

$$a = \frac{e}{m}\left[\left(\frac{\psi_c}{2\pi r_a}\right)^2 - \left(\frac{r_a B}{2}\right)^2\right] = \frac{e}{m}\frac{B^2 r_a^2}{4}\left[\left(\frac{r_b}{r_a} g_2\right)^2 - 1\right] . \tag{157}$$

As a must be zero, we have that

$$g_2 = \frac{r_a}{r_b}$$

or

$$\psi_c = \pi r_a^2 B \ . \tag{158}$$

The flux linking the cathode is just that inside the beam in the uniform section. This condition will be approximated closely when the shielded gun is immersed in a uniform axial field of density B extending over the entire system, and the pole pieces are so constructed that any flux lines at radius greater than r_a go through the outer pole piece.

In this particular case the electrons in the inner shell do not cross field lines and have no average angular velocity. This conclusion is consistent with the absence of a radial electric force at this radius. Electron shells of radius greater than r_a do cross field lines and rotate to balance the space-charge forces. No more magnetic field is used than is necessary just to counteract the space-charge force. This arrangement is considerably more efficient than that discussed in the previous division, from the standpoint of magnetic field economy.

With Eq. 158 satisfied, we have

$$B_{eff.}^2 = B^2 \left(1 + \frac{r_a^2}{r_b^2} \right) \tag{159}$$

and from Eqs. 154 and 155 we obtain

$$\varphi_2 = V + \frac{e}{m} \frac{B^2 r_a^2}{4} \left[1 + \ln \frac{r_2}{r_b} \left(\frac{r_a^2}{r_b^2} - \frac{r_b^2}{r_a^2} \right) - \frac{1}{2} \left(\frac{r_a^2}{r_b^2} + \frac{r_b^2}{r_a^2} \right) \right] . \tag{160}$$

The particular case just discussed is the same as that treated by Samuel (ref. 11), Brillouin (ref. 8) and Field (ref. 9) although the latter two do not discuss a shielded gun. The cathode described by them is a cylindrical one in a magnetron structure with the outer tube extended axially. The entire system is immersed in a uniform axial magnetic field.

It is clear that the flux ψ_c linking the cathode is the same for all electrons and therefore this arrangement falls into the category under discussion. The mechanism which controls the beam current and axial velocity is different, however, from that discussed here, as the magnetic field is entirely along the cathode surface.

Magnetic Field Absent

It has been indicated earlier that it is possible to maintain a hollow electron beam with no magnetic field in the uniform section. The field in the cathode and transition regions are still necessary of course. The design

equations for this case are derivable from those of this division by setting B = 0. Thus

$$B_{eff.} = \frac{\Psi_c}{\pi r_a r_b} \tag{161}$$

$$\rho = \frac{e}{m}\frac{\varepsilon}{2}\frac{\Psi_c^2}{\pi^2 r_o^4} \tag{162}$$

$$\varphi_1 = V - \frac{e}{4m}\left(\frac{\Psi_c}{\pi r_a}\right)^2 \left(\ln \frac{r_a}{r_1} + \frac{1}{2}\right) \tag{163}$$

$$\varphi_2 - \varphi_1 = \frac{e}{4m}\left(\frac{\Psi_c}{\pi r_a}\right)^2 \left[\left(\ln \frac{r_a}{r_1} + \frac{1}{2}\right) + \frac{r_a^2}{r_b^2}\left(\ln \frac{r_2}{r_b} - \frac{1}{2}\right)\right] . \tag{164}$$

The charge distribution in the beam is concentrated quite heavily on the inside as (162) shows. This particular charge distribution is the only one that can produce a space-charge field of the proper form to balance the centrifugal forces encountered. This may be seen by consideration of (27) in the limit when K is infinite, and then solving for α. The result makes it apparent that the charge density varies as $1/r_o^4$.

This case may appear strange at first sight as it is a degenerate form of magnetic focusing. The physical explanation lies in the fact that $\varphi_2 - \varphi_1$ is negative. An inward radial electric force is present and this force more than overcomes the outward space-charge force. Electrons leaving the gun cross magnetic field lines to get out of the field and in doing so they acquire a rotational velocity about the axis. The centrifugal and space-charge forces just balance the applied electric field. The beam cannot spread because it does not have enough energy, and it cannot collapse because it must conserve its angular momentum. A mechanical analogue is that of a ball spinning around the sides of a bowl in a gravitational field. The same balance of forces keeps the ball at some radius midway up the sides of the bowl.

The practical significance of this case is quite evident. Not only is there a very great saving in power needed for magnetic fields, but the main coils and power supplies may also be eliminated. Mechanical alignment between the magnetic field and electrodes is no longer a problem and the tube may be connected to radio-frequency apparatus much more simply than usual.

The particular charge distribution obtained may be considered a severe limitation, but in some cases it can be turned to advantage. In a coaxial type of traveling-wave tube, for example, this kind of charge distribution would be very efficient if the inner electrode were corrugated to slow the

wave, rather than the outer one.

There is one more particular case that may be classified in this division. That is the one where the magnetic flux linking the cathode is zero. If ψ_c is set equal to zero in the general equations for this group, we obtain results identical to those presented in division I. The two categories have this one case in common.

A word of precaution is indicated here. In all of division II the charge density is not uniform. Pierce guns, however, have the characteristic of using the cathode surface equally efficiently over its entire area, and the charge density of the beam leaving the gun is uniform. In the transition region, therefore, there is a shift of charge density toward the inside and constant radius trajectories are impossible for all but the innermost electrons. The shift is not a particularly violent one but it is probably enough to invalidate many of the remarks of sec. V.

On the other hand, when shielded electron guns are used, the transition region is likely to be very short and not susceptible to design. In a short space it is unlikely that electrons can be violently displaced, and if the beam enters the drift tubes and uniform beam section immediately after the transition, it should remain well focused.

It is also to be noted that since the charge density is nonuniform, the frequency β is not independent of r_o and the assumption that electrons do not cross radially is unjustified. This is of concern only when oscillations take place; the conclusions about the equilibrium state are completely valid. In developing these design equations we have done more than just to balance the radial forces. We have also specified the energy of the particles. If we had taken a more direct approach and balanced the radial electric, the centrifugal, and the magnetic forces, we would have obtained the same design equations for the charge density, magnetic field strength, and difference between electrode voltages. The equation for the actual voltage of the inner electrode $\varphi_1 - V$, however, is based on the energy balance. It is possible to have the proper electric field for focusing, but its integral, the potential, may be the wrong value.

In division I where the field at the cathode is uniform, the potential γ does not have the proper functional form, while in division II it does. In both cases, the radial field does have the required form as a function of radius.

The following table summarizes the design formulae developed in this section. They are brought together for convenient reference.

Table of Design Formulae

For all cases $B_{eff.}^2 = \dfrac{6.9 \times 10^{-7}}{r_b^2 - r_a^2} \dfrac{I}{\sqrt{V}}$

I. $\Psi_c = \pi r_o^2 B_c$

General

$$B_{eff.}^2 = B^2 - B_c^2 = B^2(1 - g_1^2) \qquad B_c = g_1 B$$

$$\varphi_1 = V + \frac{e}{m}\frac{r_a^2}{4} B^2 \left[(1 - g_1^2) \ln \frac{r_a}{r_1} + \frac{3}{2} g_1^2 - g_1 - \frac{1}{2} \right]$$

$$\varphi_2 - \varphi_1 = -\frac{e}{m}\frac{r_a^2}{4} B_{eff.}^2 \left[\left(\ln \frac{r_2 r_a}{r_1 r_b} - \frac{1}{2} \right) + \frac{r_b^2}{r_a^2} \left(\ln \frac{r_2}{r_b} + \frac{1}{2} \right) \right]$$

$$\delta = -\frac{e}{m}\frac{B^2}{4} g_1 (1 - g_1)(r_o^2 - r_a^2)$$

$$x^2 = \frac{2g_1(1 - g_1)}{(1 + g_1^2)} \left(1 - \frac{r_a^2}{r_o^2} \right)$$

$B_c = 0$

$$B_{eff.}^2 = B^2$$

$$\varphi_1 = V + \frac{e}{m}\frac{r_a^2}{4} B^2 \left(\ln \frac{r_a}{r_1} - \frac{1}{2} \right)$$

$$\varphi_2 - \varphi_1 = -\frac{e}{m}\frac{r_a^2}{4} B^2 \left[\left(\ln \frac{r_2 r_a}{r_1 r_b} - \frac{1}{2} \right) + \frac{r_b^2}{r_a^2} \left(\ln \frac{r_2}{r_b} + \frac{1}{2} \right) \right]$$

Solid Beam

$$\varphi_2 = V - \frac{e}{m}\frac{B^2 r_b^2}{4} \left(\ln \frac{r_2}{r_b} + \frac{1}{2} \right)$$

II. Ψ_c Independent of r_o

General

$$B_{eff.}^2 = B^2 + \left(\frac{\Psi_c}{\pi r_a r_b} \right)^2 \qquad \frac{\Psi_c}{\pi r_a r_b} = g_2 B$$

$$\varphi_1 = V + \frac{e}{m}\frac{B^2}{4} r_a^2 \left[\ln \frac{r_a}{r_1} \left(1 - \frac{r_b^2}{r_a^2} g_2^2 \right) - \frac{1}{2} \left(g_2 \frac{r_b}{r_a} - 1 \right)^2 \right]$$

$$\varphi_2 - \varphi_1 = \frac{e}{m}\frac{B^2 r_a^2}{4}\left[g_2^2\frac{r_b^2}{r_a^2}\left(\ln\frac{r_a}{r_1}+\frac{1}{2}\right)+g_2^2\left(\ln\frac{r_2}{r_b}-\frac{1}{2}\right)\right.$$

$$\left.-\left(\ln\frac{r_a}{r_1}-\frac{1}{2}\right)-\frac{r_b^2}{r_a^2}\left(\ln\frac{r_2}{r_b}+\frac{1}{2}\right)\right]$$

$\varphi_2 = \varphi_1$

$$g_2 = \left[\frac{\left(\ln\frac{r_a}{r_1}-\frac{1}{2}\right)+\frac{r_b^2}{r_a^2}\left(\ln\frac{r_2}{r_b}+\frac{1}{2}\right)}{\frac{r_b^2}{r_a^2}\left(\ln\frac{r_a}{r_1}+\frac{1}{2}\right)+\left(\ln\frac{r_2}{r_b}-\frac{1}{2}\right)}\right]^{\frac{1}{2}}$$

Inner Electrode Absent

$$g_2 = \frac{r_a}{r_b} \qquad B_{eff.}^2 = B^2\left(1+\frac{r_a^2}{r_b^2}\right)$$

$$\varphi_2 = V + \frac{e}{m}\frac{B^2 r_a^2}{4}\left[1+\ln\frac{r_2}{r_b}\left(\frac{r_a^2}{r_b^2}-\frac{r_b^2}{r_a^2}\right)-\frac{1}{2}\left(\frac{r_a^2}{r_b^2}+\frac{r_b^2}{r_a^2}\right)\right]$$

B=0

$$B_{eff.}^2 = \left(\frac{\Psi_c}{\pi r_a r_b}\right)^2 \qquad \varphi_1 = V - \frac{e}{4m}\left(\frac{\Psi_c}{\pi r_a}\right)^2\left(\ln\frac{r_a}{r_1}+\frac{1}{2}\right)$$

$$\varphi_2 - \varphi_1 = \frac{e}{4m}\left(\frac{\Psi_c}{\pi r_a}\right)^2\left[\left(\ln\frac{r_a}{r_1}+\frac{1}{2}\right)+\frac{r_a^2}{r_b^2}\left(\ln\frac{r_2}{r_b}-\frac{1}{2}\right)\right]$$

VII. THE EFFECTS OF RESIDUAL GAS

So far, the systems discussed have been assumed to exist in an essentially perfect vacuum. Frequently this assumption is reasonably accurate but it sometimes happens that the small amount of residual gas in the tube has a serious effect on the behavior of the beam.

This disturbing effect is not a scattering due to many collisions. Unless the tube is defective or poorly outgassed and pumped, the vacuum is always sufficiently high to make the probability of collision negligibly small. Nevertheless, there are always some collisions with the consequent production of secondary electrons, positive or negative ions. The positive ions, if not somehow removed, may collect in the region of the beam and affect the net space charge. The resulting change in the spatial potential distribution is responsible for the disturbance of the beam's behavior. In cathode-ray tubes, for example, this positive-ion production produces a partial neutralization of

the electron-beam space charge and a resultant improvement in the focusing. This effect is not to be confused with gas focusing which actually concentrates the beam into a thin pencil rather than just reducing the spread, and which does not occur except at considerably higher pressures than those usually used.

It would be of interest to learn whether any of these effects are likely to be significant in magnetically focused beams and what forms they might take. Since only a finite goodness of vacuum can be achieved, it is inevitable that some ions will be produced. We shall consider this problem here and its relation to our design methods. It is necessary to make many assumptions as there are many unknown quantities. This analysis must therefore be qualitative only. Various factors are considered but their relative importances are not evaluated.

In what follows, the same notation as used previously is continued except for the symbols e and m, which are used to denote the charge and mass of whichever particles are being discussed.

Consider an electron in a shell of radius r_o colliding with a molecule of gas. This collision results in the formation of a secondary electron and a positive ion. The primary electron recoils in some undetermined direction. We assume that the energy lost by the primary electron is just about the ionization energy which is of the order of 15 electron-volts. The recoil velocity of the primary electron is thus almost equal to its original velocity. The initial velocities of the products of collision are zero, according to the assumption above.

Since the scattered primaries have appreciable velocities, they do not remain in any one region of the tube, and since we are assuming a fairly good vacuum, there is not a sufficient concentration of primaries to affect the situation seriously. We cannot neglect the secondary electrons or positive ions because of their low velocities.

For electrons or ions originating at r_o with zero velocity the energy equation corresponding to (1) is

$$\dot{r}^2 + r^2\dot{\theta}^2 + \dot{z}^2 = -2\frac{e}{m}(\varphi - \varphi_o) \tag{165}$$

where φ_o is the electrostatic potential at r_o where the ions originate; φ_o is the same as γ_o. The angular momentum equation corresponding to (9) is

$$\dot{\theta} = \frac{e}{mr^2}(r_o A_o - rA_\theta) \tag{166}$$

where A_o is the vector potential at radius r_o. Equation 166 may be simplified because we are working in a uniform magnetic field.

$$\dot{\theta} = \omega_H\left(\frac{r_o^2}{r^2} - 1\right). \tag{167}$$

This is an equation commonly used in connection with magnetrons.

Substituting (167) into (165) setting $\dot{z} = 0$ and rearranging, we get

$$\dot{r}^2 = -2\frac{e}{m}(\gamma - \gamma_o) - \omega_H^2 r^2 \left(\frac{r_o^2}{r^2} - 1\right)^2 . \qquad (168)$$

A graph of the second term on the right hand side of (168) has the general form shown in Fig. 14. The zero value at $r = r_o$ persists even when the first term is added to it, since γ at r_o is by definition γ_o. The first term has the effect of adding another root to the equation $\dot{r}^2 = 0$ thereby defining a region between r_o and this second root where the electrons or positive ions may travel. If the term $-2\ e/m\ (\gamma - \gamma_o)$ increases with r_o this second root is at a value of r greater than r_o and vice versa. In any case, the positive ions and electrons move in separate regions, both bounded by r_o.

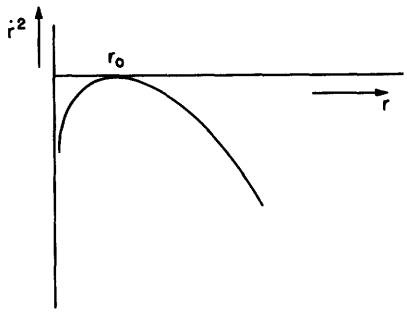

Fig. 14 The last term of Eq. 168.

In order to put this question on a somewhat more quantitative base, we proceed as in sec. II in the derivation of the small-signal solution. Letting $R = r^2$ and adding the expressions for $\dot{r}^2$ and $\ddot{r}$ as before, we obtain

$$\ddot{R} = -4\frac{e}{m}(\gamma - \gamma_o) - 4\,\omega_H^2 r^2 + 4\,r_o^2\omega_H^2 - 2\frac{e}{m}\,r\,\frac{\partial\gamma}{\partial r} . \qquad (169)$$

In order to simplify this equation we let

$$\gamma - \gamma_o = \Gamma(r^2 - r_o^2) \quad \text{or} \quad \gamma = \Gamma r^2$$

$$\frac{\partial\gamma}{\partial r} = 2\Gamma r \qquad (170)$$

then

$$\ddot{R} = \left(-8\frac{e}{m}\Gamma - 4\,\omega_H^2\right)R + 4\left(\frac{e}{m}\Gamma + \omega_H^2\right)R_o . \qquad (171)$$

The solution to this equation is easily obtained and after simplification it becomes

$$\frac{R}{R_o} = \frac{1 + L}{1 + 2L} - \frac{L}{1 + 2L}\cos 2\omega_H\sqrt{1 + 2L}\,t \qquad (172)$$

where

$$L = \frac{e/m\,\Gamma}{\omega_H^2} = \frac{4\Gamma}{e/m\,B^2} . \qquad (173)$$

This solution is valid only for the special case where Eq. 170 is true, otherwise it is valid only for small oscillations about $R/R_o = 1$ where Eq. 170 is a good approximation. In any case it corroborates the previous conclusions about the separation of electrons and positive ions.

The ranges of oscillation of R/R_o are between the values of 1 and $1/1 + 2L$

so that L must be greater than - 1/2. The sign of L depends on the particle concerned and on the sign of Γ which is the same for all particles. Consequently $1/1 + 2L > 1$ for one particle and < 1 for the other. The magnitude of L depends on the value of e/m for the particle concerned. L is very much greater for the heavy positive ions than for electrons and consequently these ions have a range of oscillation much greater than that of the electrons. Even though the quantitative analysis presented here might not hold in most cases, the qualitative aspects are the same and it is quite conceivable that the positive ions may be removed from the beam by colliding with one of the electrodes. The situation is shown in Fig. 15.

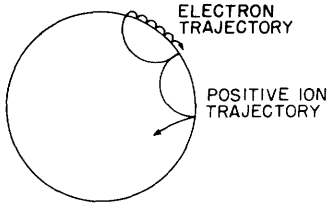

Fig. 15 Separation and relative magnitudes of ion and electron trajectories.

If the assumption of zero initial velocities is not true but the ions do have a small initial velocity, then our conclusions as to the motion of the particles are not seriously affected. Instead of following paths which resemble cycloids, the particles will follow trochoidal paths of essentially similar dimensions.

It is thus quite possible that the positive-ion removal due to the magnetic field may predominate. The trapping of electrons may increase rather than decrease the effect of space charge.

Initial velocities of the products of ionization in the axial direction on the other hand increase the relative loss of electrons since they have the larger initial velocity.

If positive ions are trapped as well as electrons, another effect comes to notice. The ranges of oscillation for particles of opposite charge lie on opposite sides of the radius where the particles originate. Small initial velocities cause a certain amount of overlapping but the sorting action is still present. The products of ionization from any shell are separated and form a dipole layer. The polarity of this dipole layer is such as to reduce the potential gradient in the beam. Even though the superposed charge densities inside the beam due to each dipole layer may be zero, the resultant moment of the unneutralized layers at the edges of the beam are the same as though each were considered separately and the results added.

This reduction of radial electric field in the beam is a self-stabilizing process since it works for either direction of field. We might, therefore, expect to find that any radial electric field in the beam is cancelled by the effects of incidental ionization. When this happens, α becomes zero and we must make ψ_c equal to ψ. The entire system can then be immersed in a uniform magnetic field and the voltages on both inner and outer electrodes may be made the same. In effect the space-charge *plus* the charges on the electrodes have

been cancelled by the ionization and the magnetic field.

The effects described above have not been shown to be certain to occur; they have only been shown to be possible. Before leaving the consideration of the effects of ionization, we shall look into one more situation.

In electron beams without magnetic fields there is a potential depression in the beam. This depression acts as a trough or trap for positive ions and consequently the common effect of incidental ionization in these cases is neutralization of the space charge. Although we have no definite reason to expect that this same sort of neutralization will occur in magnetically focused beams, it may be informative to consider its consequences if it does occur.

If there is complete space-charge neutralization, the charge density is zero regardless of the beam current. As there are no dispersive forces, focusing is not required. The magnetic field can be zero or any other value if we maintain the field uniform over the entire system. The electrode voltages are just set at that corresponding to the axial velocity. The inner electrode may be omitted if desired.

If the whole system is immersed in a uniform field, electrons do not cross field lines and there is no rotation of the beam. While the magnetic field is not necessary, it does serve the purpose of keeping the beam focused. Without it the initial velocities of all electrons as they enter the drift tubes would have to be axial. Small errors in this matter are controlled by the field if it is used.

This section completes the theoretical part of this paper. The remainder is devoted to a discussion of some experiments performed to verify some of the theory presented.

VIII. DESCRIPTION OF EXPERIMENTS

A series of experiments were performed to check some of the theory that has been presented. This section contains a description of the apparatus and methods used in these tests. The results obtained are discussed in the next section and will not be mentioned here except for the way in which partial results guided the experimental work.

In all of these experiments the same beam parameters were used, along with the same drift tubes and electron guns. The differences between the various tests lay in the cathode flux conditions, magnetic field intensities and electrode voltages. The specific conditions used were based on some of the special cases discussed in sec. VI.

In choosing the voltage V, currentI, and dimensions of the electron beam, a compromise was made between the charge density in the beam and the current

density available from oxide-coated cathodes. Large radii were chosen so that slight inaccuracies and asymmetries in construction would be relatively unimportant. The beam density was set sufficiently high so that it would have to be taken into account in the design. It was decided to use an electron gun which produced a beam of the desired final dimensions and the cathode area was the same as the beam cross-sectional area. This placed a limit on the current density. An emission density of 150 ma/cm^2 was chosen as a conservative value which could easily be obtained. The beam parameters selected on the above considerations are listed below.

Inner radius	r_a	1.125 cm
Outer radius	r_b	1.525 cm
Beam voltage	V	1000 volts
Beam current	I	500 ma

The electron gun was designed to operate with this same current and voltage. The beam inside the gun was a constant radius one, as shown in Fig. 13, and therefore could be considered as an annulus cut from the flow in an infinite parallel-plane diode. The corresponding potential distribution and the necessary spacing between cathode and anode are easily calculated, and the remainder of the design was carried out in the electrolytic tank. This design is the straightforward Pierce method where the shapes of the electrodes necessary to produce the required beam are determined. For the hollow beam, two strips of dielectric had to be used, one for the inner and one for the outer edges. The design of the inner and outer shaped electrodes were carried out independently of each other. Figure 16 is a photograph of one of the electron guns and the cathode is shown separately with the beam-forming electrodes around it. The projecting rod and large-diameter tube shown here are not parts of the gun proper but are associated with the transition region. The anode of the gun is just a flat plate to which these projections are attached.

Heaters for these cathodes required considerable developmental work. They were finally wound from 0.007" tungsten wire on a jig with spiral grooves cut in a plane. The winding is a bifilar one to minimize the effects of the magnetic field of the heater current itself which ran about 2 amperes. The heater power required for these large cathodes was about 40 watts.

The dimensions of the drift tubes are such that about 3 mm clearance on each side of the beam is obtained. The length was chosen long enough to insure that only a properly focused beam would pass through it, and short enough to insure that it would lie entirely in the uniform field of the fifteen-inch solenoid used. The dimensions of the drift tubes, which were made of sheet tantalum spot-welded around a mandrel, are shown next.

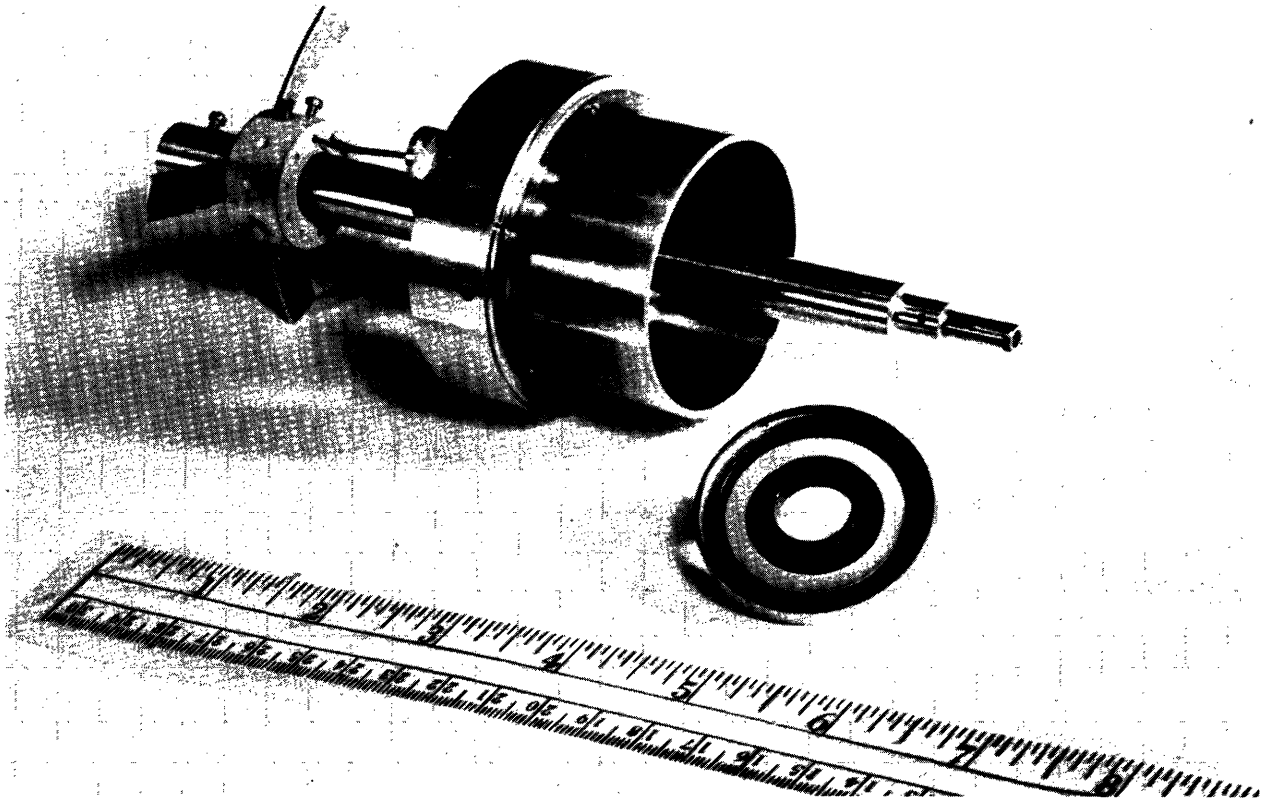

Fig. 16 Electron gun and cathode assembly.

Radius of inner drift tube	r_1	0.800 cm
Radius of outer drift tube	r_2	1.825 cm
Length of both tubes		7 inches

At the end of the drift tubes a deep collector cup was used. In order to prevent any disturbance of the beam as it left the drift tube the collector cup was divided into three parts; the inner collector tube, the outer collector tube, and the collector plate. The two collector tubes, each two inches long, were just extensions of the drift tubes. Each collector tube was held at the same potential as the corresponding drift tube but insulated from it so that the currents to each could be measured separately. The collector plate or ring closed off the end of this section and this electrode was held at 45 volts above whichever drift tube had the higher potential. The purpose of this bias voltage was to collect any secondary electrons that might be released by the beam striking any of the electrodes in the vicinity.

The arrangement of the drift tubes and collector assembly are shown in Fig. 17 and the actual tubes are pictures in Fig. 18. The flanges on the sides of the tubes are for centering the entire assembly in a glass tube.

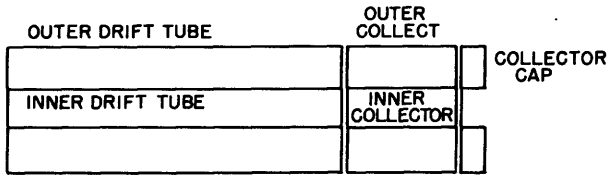

Fig. 17 Drift tube and collector arrangement.

All of the experiments were done in a continuously pumped demountable vacuum system. The vacuum chamber was a long brass tube, capped with a brass plate at one end and attached to a brass pumping head at the gun

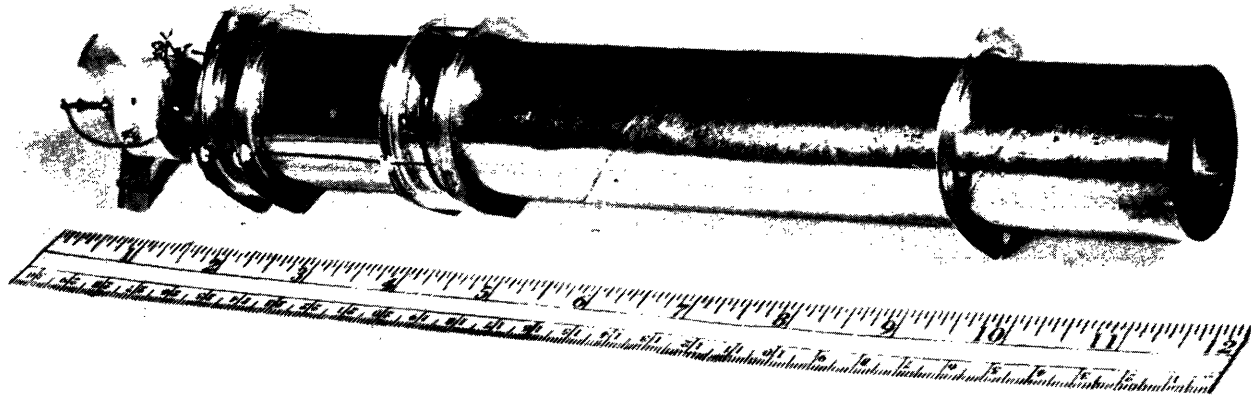

Fig. 18 The drift tube and collector assembly.

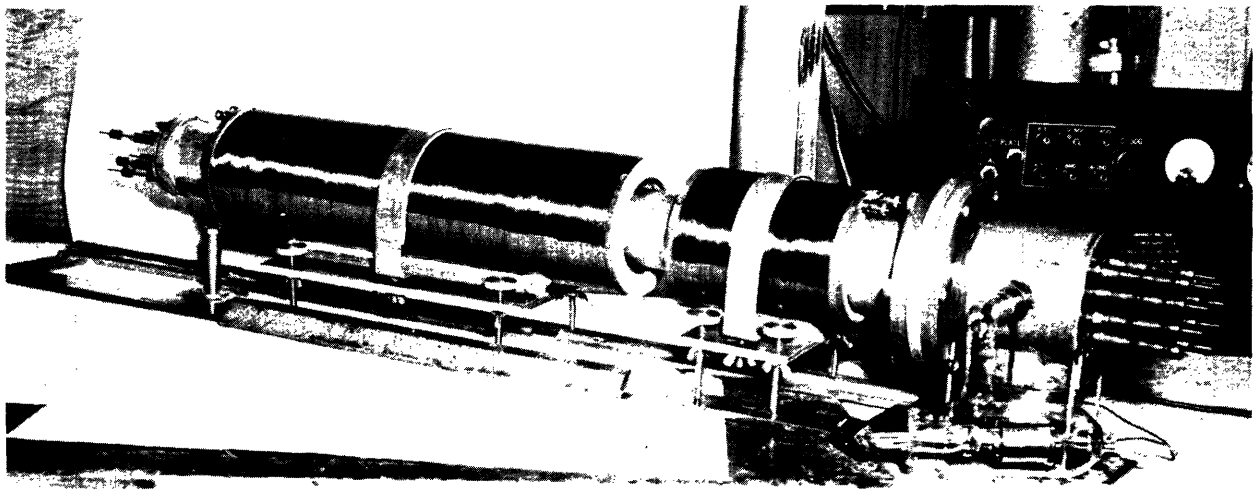

Fig. 19 Vacuum system and solenoids.

end. Leads were brought through both ends of the system and the vacuum seals were made with rings of solder, butt-soldered and filed to form a smooth gasket. The vacuum system with the magnet coils around it is pictured in Fig. 19. This system was capable of producing a vacuum of about 10^{-7} mm of mercury after several days pumping, but all the experiments were done at pressures of 1 to

4×10^{-6} mm Hg.

The power supply and measuring circuits were standard except that the tube was pulsed by driving the cathode negative with respect to the gun anode. The purpose of the pulse system was to reduce the power dissipation required at the collector. A duty ratio of 0.01 was obtained with twenty microsecond pulses at a repetition rate of 500 pulses per second. A synchroscope was used to trigger a pulse generator which modulated a magnetron power supply. As shown in the block diagram of the circuit, Fig. 20, the synchroscope was also used to observe the shape of the pulse applied to the cathode.

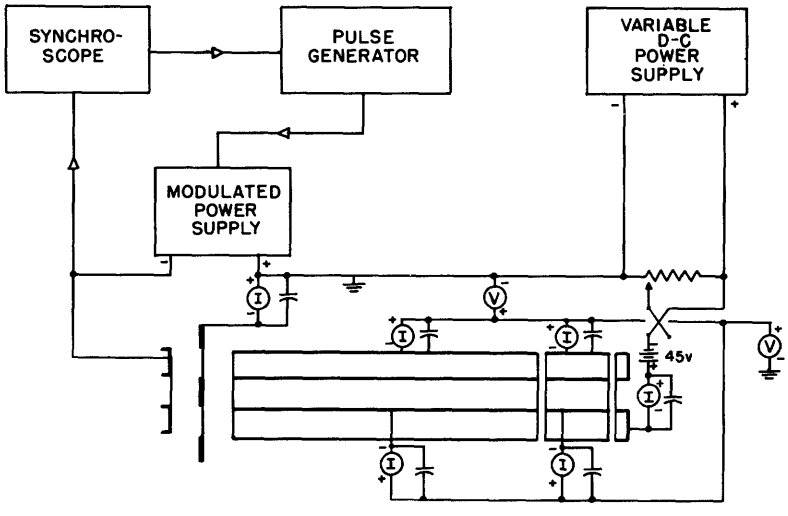

Fig. 20 Measuring circuit.

The voltages applied to the drift tubes and collectors were obtained from a d-c supply and the currents were measured with ordinary d-c panel meters calibrated for increased accuracy. By-pass condensers placed across each meter insured a correct reading of average current. The measurements were taken point by point and require no further comment.

There is nothing special about the solenoids used for the magnetic field either. They were both wound with ten layers of wire on bakelite forms. Their average diameter was 4 inches. One coil had a winding 15 inches long and the other was 5 inches long, otherwise they were identical. The long coil produced a field of 85 gauss/ampere at its center and the short one, 71.6 gauss/ampere at its center. For a description of the measuring apparatus and calculations used with these coils, the reader is referred to the appendix.

In all, four different tubes were constructed and tested. Of these, the third and the fourth were almost identical and gave almost identical results. They will therefore be described together.

Tube 1 was built with a gun made of nonmagnetic materials and was operated with the cathode in the center plane of the five-inch solenoid. The currents in the two solenoids could be adjusted independently and it was intended to operate this tube under the conditions described in division I of sec. VI, i.e. with the cathode in a uniform field of value B_c.

This tube had a transition region of very crude design based on the

following reasoning. The values of B_c to be used were 0 and $\frac{1}{2}B$. For each of these configurations the magnetic field intensity along the axis was plotted using the curves shown in the appendix. These results are shown in Figs. 21 and 22. Examination of these curves shows the transition region to be about five inches long, so the drift tubes were spaced five inches from the anode of the gun. The radial gradient which depends on the quantity $\psi^2 - \psi_c^2$ is greatest near the drift tubes and decreases toward the anode of the gun. This field is almost of the type that might be formed by the fringing at the end of the drift tubes, but a fringing field would drop too rapidly along the axis. To help extend it a two-inch tube the same radius of the inner drift tube was set in the transition region near the drift tubes. A separate lead was brought to this tube so that its potential could be adjusted. The arrangement is shown in Fig. 23.

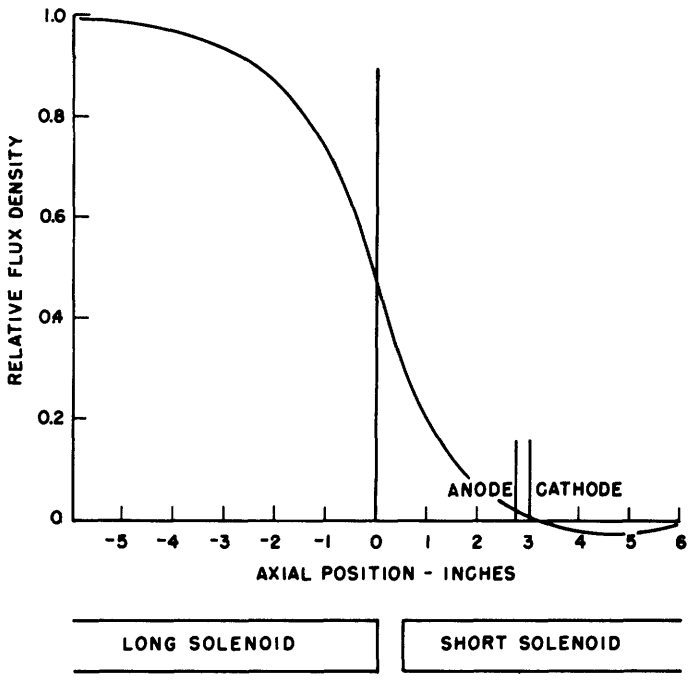

Fig. 21 Magnetic field configuration with $B_c = 0$.

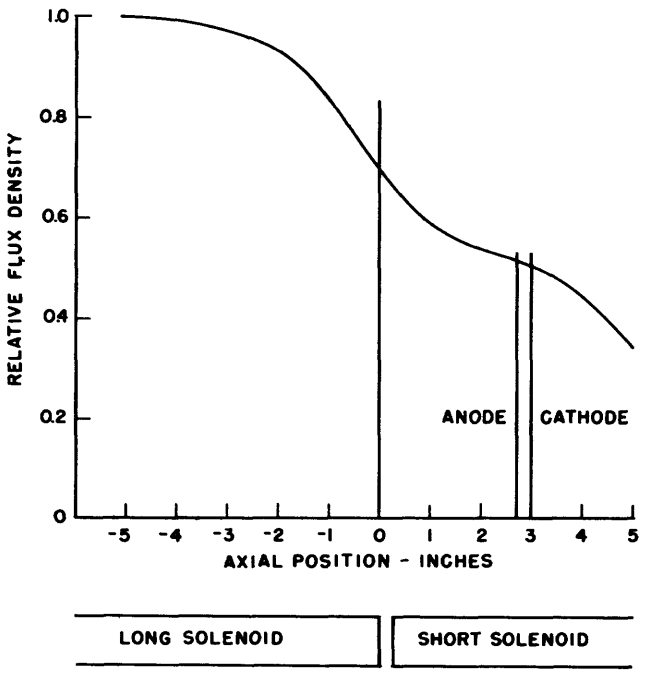

Fig. 22 Magnetic field configuration with $B_c = \frac{1}{2}B$.

As will be noted in the next section, this tube worked very well with $B_c = \frac{1}{2}B$ but not at all with $B_c = 0$. Consequently some effort was expended on the design of a transition region so the tube could be used with $B_c = 0$. The tube with transition region will be called tube 2. Aside from this one difference, it was identical with tube 1.

The method of design used for this transition region was different from that outlined in sec V. An attempt was made to eliminate the effects of space charge by

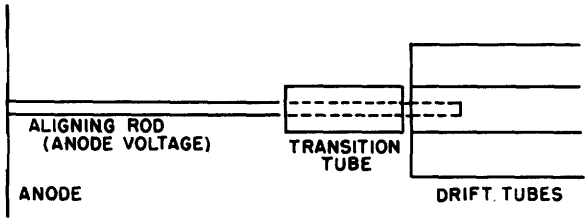

Fig. 23 Transition region in tube 1.

calculating the radial electric field in the uniform section of the beam under the proper design conditions. The field was again calculated with the beam absent but with the same potentials applied to the drift tube. These two fields were equated and the resulting equation solved for the radius at which there was no error in neglecting the space charge. This radius was then used through the entire transition region in the model set up in the electrolytic tank.

A series of probe pairs were set along this radius in the tank, the separation in each pair being radial. Extensions of the inner and outer drift tubes and of the anode were adjusted in size and shape until each probe pair registered the required potential difference.* It is to be noted that while the gradient could be adjusted reasonably well, there were quite violent fluctuations in the actual potential along the test radius.

The electrodes resulting from this procedure are shown diagrammatically and not to scale, in Fig. 24.

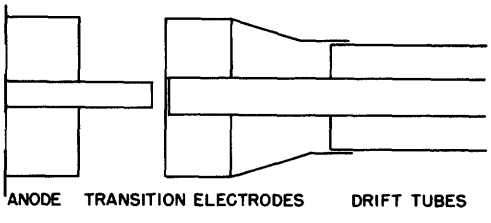

Fig. 24 Transition region for $B_c = 0$ tube 2.

The third and fourth tubes were built to test the possibility of focusing the electron beam without a magnetic field along the uniform section. This requires the use of a shielded electron gun as explained in sec. VI. The gun used is pictured in Fig. 25. All the parts except the cathode and beam-shaping electrodes were made of cold-rolled steel. The center post was extended and joined across the back of the gun to the outer anode rim by means of steel posts. The resulting magnetic circuit was activated by the brass enclosed coil mounted on the center post. The entire construction is similar to that of a dynamic loudspeaker magnetic circuit, and the radial flux across the anode gap is the essential part of the system.

With this electron gun the drift tubes were placed close to the anode, without any shaping of the ends of the tubes. The only difference between tubes 3 and 4 was the thickness of the anodes. The reason for this difference will be made clear in the next section as we consider the results of the experiments outlined here.

---

*The author is indebted to Mr. Herman Haus for carrying out the actual tank design.

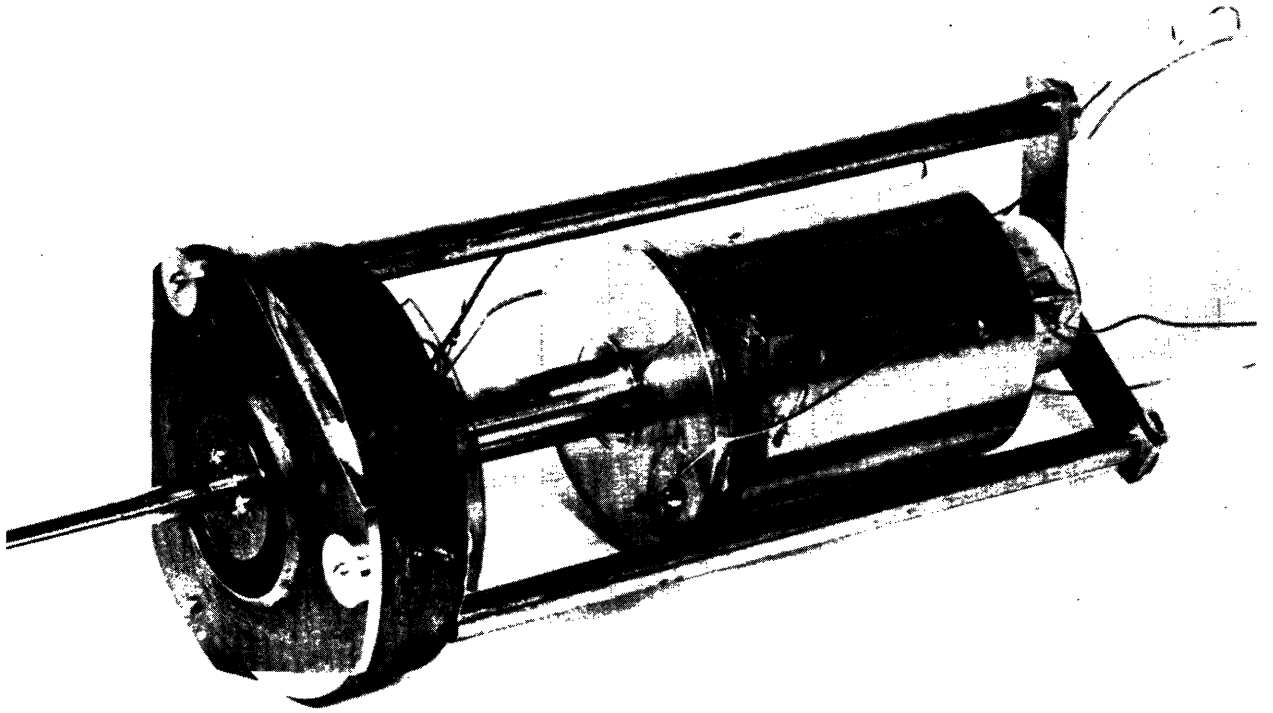

Fig. 25 The shielded electron gun.

IX. EXPERIMENTAL RESULTS

In this section the results of the experiments just outlined are presented for the most part in the form of graphs of the current to the various electrodes in the tube. These measurements were taken point by point, holding all parameters constant except one. The collector current indicated on the graphs is the sum of all the current going to the three final electrodes.

Before considering the specific results in detail it is to be noted that as they are shown, there are more factors involved than those indicated explicitly on the graphs. There are so many variables that it is almost impossible to hold all except one constant with the experimental arrangement used here. The standard of performance adopted here was the value of collector current relative to the drift tube currents. This value could stay constant while the beam changed dimensions within the limits of the drift tubes, or changed its axial velocity, or even changed its charge distribution and axial velocity distribution. These facts should be borne in mind when the graphs of performance are examined. The most important of these "hidden" factors will be seen to be the performance of the transition region.

When the electron beam does not penetrate this region properly, the result is a large increase in drift tube currents with a corresponding decrease

in collector current, a change which can also be interpreted as poor focusing of the beam itself.

In what follows, the following notation is used, both in the text and on the graphs:

Collector current	I_c
Inner drift-tube current	I_1
Outer drift-tube current	I_2
Anode current	I_a
Inner drift-tube voltage	φ_1
Outer drift-tube voltage	φ_2
Current in long solenoid	I_{15}
Current in short solenoid	I_5
Current in coil on shielded gun	I_G

The anode voltage with respect to the cathode was 1000 volts for all the experiments and the axial velocity was assumed to correspond to this same voltage.

Tube 1

This tube was operated with $B_c = B/2$. It was determined experimentally that the best results were obtained from the transition region when the transition tube was held at anode potential (Fig. 23). The calculated design voltages and solenoid currents for this tube are listed below.

φ_1	1282 volts
φ_2	2012 volts
I_{15}	1.380 amperes
I_5	0.685 ampere

The curves of Fig. 26 show the effects of varying the inner and outer drift-tube voltages separately with the magnetic field held constant. As we would expect the beam radius decreases with increasing φ_1 as evidenced by the decrease in I_2 followed by the increase in I_1. In between where the drift-tube currents are a minimum, the collector current is a maximum. Similarly the beam radius is seen to be small when φ_2 is low and it increases as the radial gradient is increased. The irregularities near the value of φ_2 equal to that of φ_1 may be caused by a change in the action of the transition region, or by a redistribution of current due to secondary electrons released from the drift tubes.

The very broad maxima in both curves of collector current may be attributed to the rather large clearance between the beam and drift tubes which allowed the beam considerable change in radius before it could fail to reach the collector.

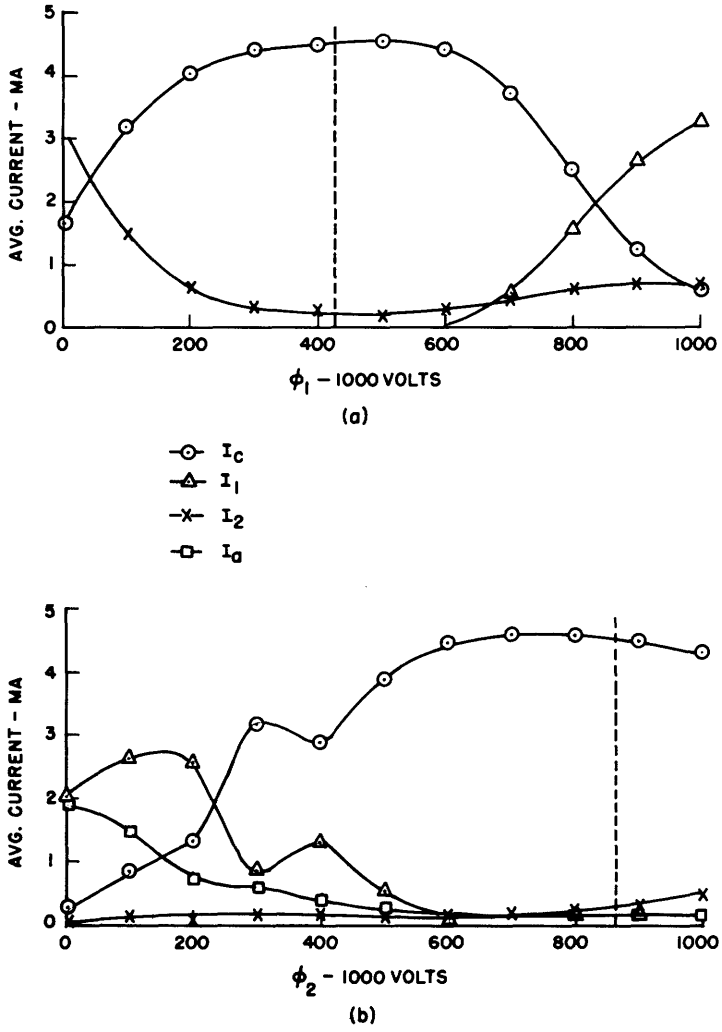

Fig. 26 Focusing as a function of drift-tube voltages, tube No. 1 - I_{15} = 1.380 amp, I_5 = 0.685 amp, B_c = ½B. a. φ_2 - V = 1012 volts; b. φ_1 - V = 282 volts.

A check on the pulse duration used for these curves showed that the beam current was only 400 ma rather than the 500 ma assumed. The design parameters were recalculated on this basis and it was found that the difference in voltage between the drift tubes should be

$$\varphi_2 - \varphi_1 = 585 \text{ volts}$$

rather than the 656 volts previously calculated. On this basis, with φ_2 = 2012 volts, the optimum value of φ_1 is 1427 volts as indicated by the vertical line on the top graph. With φ_1 at 1282 volts, the optimum value of φ_2 is 1867 volts as shown on the lower graph of Fig. 26. These results agree reasonably well with the theory, considering the number of factors not susceptible to measurement.

The effects of incidental ionization in this tube were not checked conclusively but it was noted that an increase in pressure from about 3 to 10 × 10^{-6} mm Hg brought about an improvement in the transition region and the current to the gun anode decreased. This behavior suggests that the loss of positive ions is less than that of electrons produced by ionization, particularly near the gun. This result is not unexpected as there is a large axial gradient in this region and most of the loss would be due to axial motion. As explained in sec. VII, the electron loss predominates in this case. Positive-ion neutralization of the beam space charge may be taking place to some extent in the uniform section too. This is suggested by the fact that the optimum potential difference between drift tubes was slightly less than that predicted theoretically. The discrepancy is so small, however, that definite conclusions as to this point are not indicated.

The effects of varying the currents in the two solenoids separately are

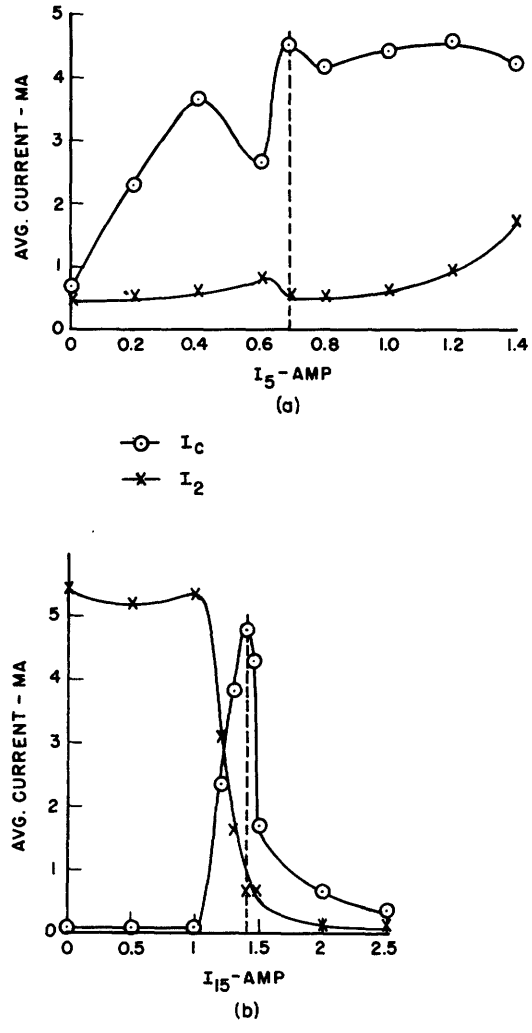

Fig. 27 Focusing as a function of relative magnetic field strengths, tube No. 1 - φ_2 - V = 1012 volts, φ_1 - V = 282 volts a. I_{15} = 1.380 amp; b. I_5 = 0.685 amp.

shown in the curves of Fig. 27. These variations caused a change in the relative values of B and B_c. The top graph of Fig. 27 shows a peak in collector current at the theoretical value of I_5, but another maximum occurs at a somewhat greater value of B_c. As conditions in the drift tubes are unchanged, this second maximum is probably due to an improved action of the transition region rather than an actual beam focusing. This curve, therefore gives us some appreciation of the relative effects of transition region and beam focusing. Note the increase of outer drift-tube current with increasing B_c. The theory indicates that the beam must expand in order to cross field lines if the magnetic field itself does not converge.

The lower curve of Fig. 27 shows how critical the relative values of magnetic field can be. With a fixed electric gradient the main focusing field must be the right value to collimate the beam. This represents a true focusing action in the uniform part of the system. If it were due to the transition region, then there would be another maximum of collector current at some lower value of I_{15} corresponding to the same magnetic field configuration as occurred with the broad maximum of the top curve. Note the sharp decrease in I_2 with increasing magnetic field strength. This action may be likened to that of the magnetron cut-off.

In developing the design formulae of secs. IV and VI, it was noted that the balance of radial forces specified the potential difference, $\varphi_2 - \varphi_1$, and the actual potential, φ_1 of the inner tube was set by energy considerations. We should expect the focusing to be relatively independent of this potential level, which primarily determines the axial velocity or amplitude of radial oscillation. This expectation is borne out by the flatness of the curves shown in Fig. 28 in which $\varphi_2 - \varphi_1$ was held constant and the value of both adjusted.

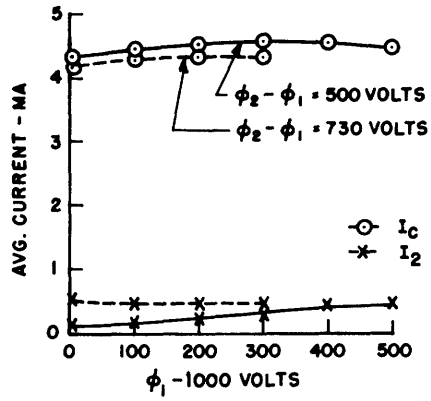

Fig. 28 Effect of beam velocity on focusing - I_{15} = 1.380 amp, I_5 = 0.685 amp, B_c = ½B.

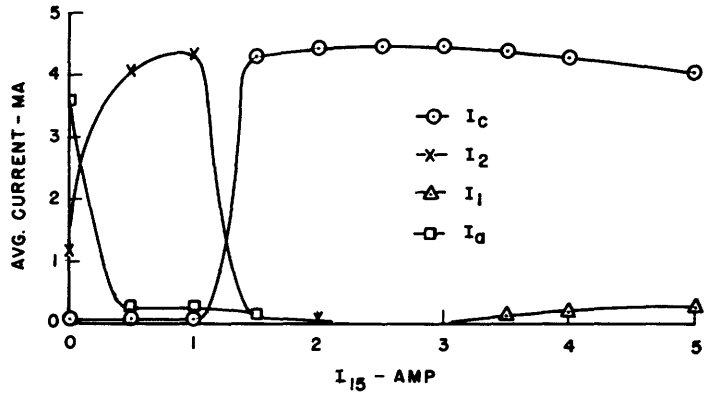

Fig. 29 Beam focusing as a function of magnetic field strength - φ_1 - 1000 = 282 volts, φ_2 - 1000 = 1012 volts, B_c = ½B.

In one other test with this tube the magnetic field strength was varied but the configuration held constant, i.e. for all values of B, B_c was held equal to B/2. The resulting curves, shown in Fig. 29, bear a striking similarity to the behavior of a magnetron with increasing magnetic field. The optimum value of I_{15} is somewhat higher than the theoretical value of 1.380 amp probably because the potential difference $\varphi_2 - \varphi_1$ was greater than it should have been. Consideration of this curve along with those of Fig. 27 makes it clear that the actual magnetic field intensity is no more critical than the electrode voltages, but the relative values of B and B_c are very critical as the cathode flux condition (Eq. 27) predicts.

Tube 2

As mentioned in the previous section, tube 1 could not be made to work at all satisfactorily with B_c = 0. No current could be made to flow to the collector and it was clear that the fault lay in the transition region. This was evidenced by the large proportions of current going to the gun anode, the centering post, and the extra transition tube. Tube 2 was built with a transition region roughly designed in the electrolytic tank for the case where B_c = 0.

The design parameters for operation under these conditions are shown in the following list.

I_{15}	1.194 amperes
I_5	-0.114 ampere
φ_2	1717 volts
φ_1	1091 volts

It was found that a total current of 350 ma was all that could be obtained

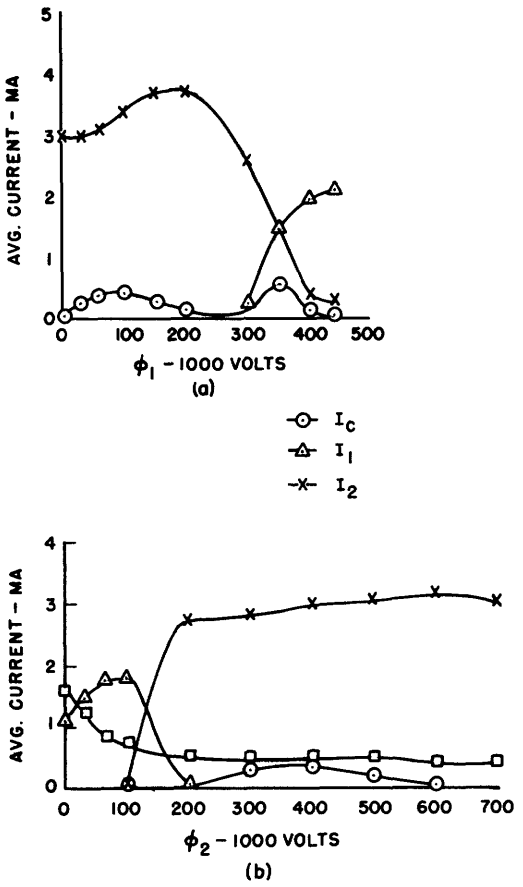

Fig. 30 Performance of tube No. 2. Design condition B_c = 0.- I_{15} = 1 amp, I_5 = -0.096 amp. a. φ_2 - 1000 = 439 volts; b. φ_1 - 1000 = 64 volts.

from this gun under these conditions the above design values were corrected for this current. The results were

I_{15}	1.00 ampere
I_5	-0.096 ampere
φ_2	1439 volts
φ_1	1064 volts

Operation with this set of values was quite unsatisfactory as shown by Fig. 30 although small maxima in the collector current curves indicate that some focusing was taking place at about the indicated voltages.

The failure of this tube is again attributed to the short-comings of the transition region. Its design is apparently far more critical than was assumed.

Since the tube could not be operated satisfactorily as designed, it was decided to find the best possible operating conditions. Once these were determined, purely empirically, the parameters were varied one by one about these optimum values. The results are shown in Figs. 31 and 32. The general character of these curves is quite similar to that of the curves obtained from tube 1, and they confirm the theory qualitatively at least. The change in beam radius with I_{15} is quite evident in Fig. 32.

The actual ratio of B to B_c used in this experiment was taken (B/B_c = 0.615) and used with the measured beam current of 450 ma to calculate the appropriate value of $\varphi_2 - \varphi_1$. This came out to be 656 volts, and from Fig. 31 the actual optimum value is about 660 volts. The actual value of φ_1 = 1060 volts does not agree so well with the calculated value of 1174 volts.

It may be noteworthy that in this experiment where the values of $\varphi_2 - \varphi_1$ agree so well, the pressure was only about 8×10^{-7} mm Hg which is considerably lower than that obtained in tube 1. This may be a confirmation of the previous indication that positive ions tend to collect in the beam and neutralize the space charge, though the evidence is far from conclusive.

One last experiment performed with tube 2 is of considerable interest. Although it does not conform to the assumptions and restrictions used in the

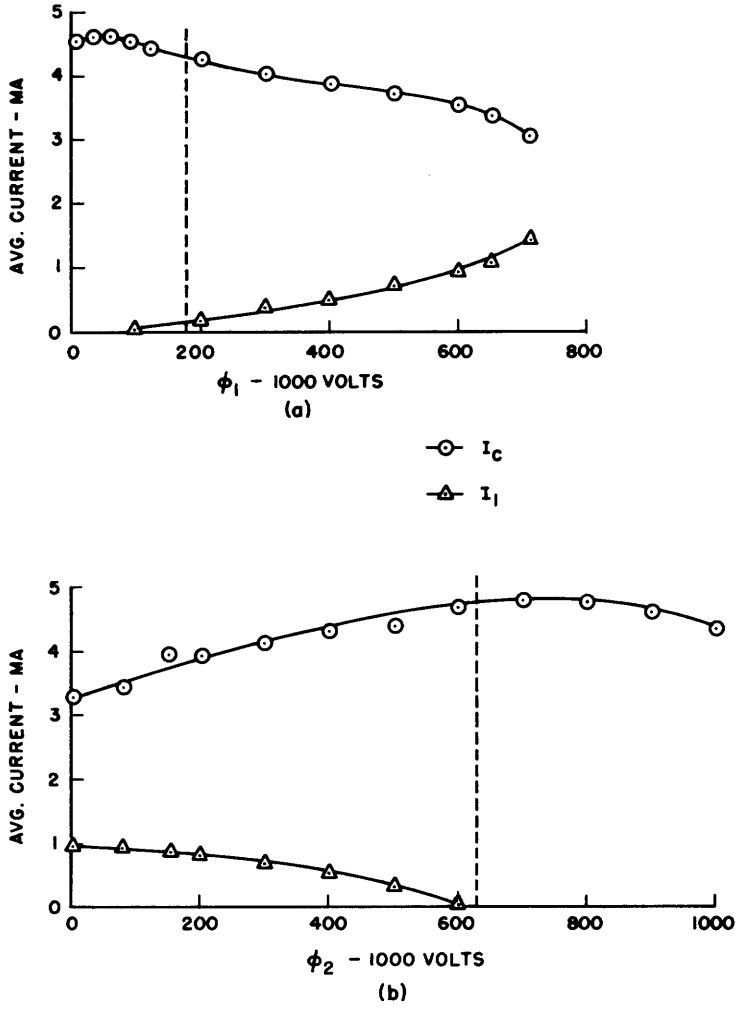

Fig. 31 Focusing as a function of drift-tube voltages, tube No. 2 - I_{15} = 1.80 amp, I_5 = 1.14 amp.
a. φ_2 - V = 710 volts; b. φ_1 - V = 80 volts.

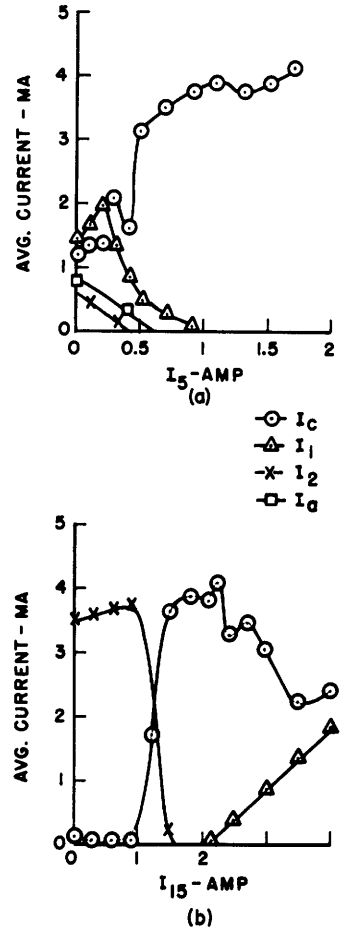

Fig. 32 Focusing as a function of relative magnetic field strengths, tube No. 2 - φ_2 - V = 710 volts, φ_1 - V = 80 volts.
a. I_{15} = 1.80 amp; b. I_5 = 1.14 amp.

theoretical analysis it illustrates the physical interpretation of the focusing process very well. In this experiment, the current in the short solenoid was held constant at 1.14 amperes while the current in the long solenoid was varied. For each value of I_{15}, both drift-tube voltages were adjusted to give the maximum collector current. The results of these measurements are shown in Fig. 33 where the upper curves represent the optimum voltages and the lower ones indicate the currents obtained with each setting.

Clearly, where the value of I_{15} is less than that of I_5, B_c is greater than B and these conditions are not in a category analyzed in this paper. For this condition, however, we do know that an inward rather than an outward electric force is required and this is seen to be the case. For the lower values

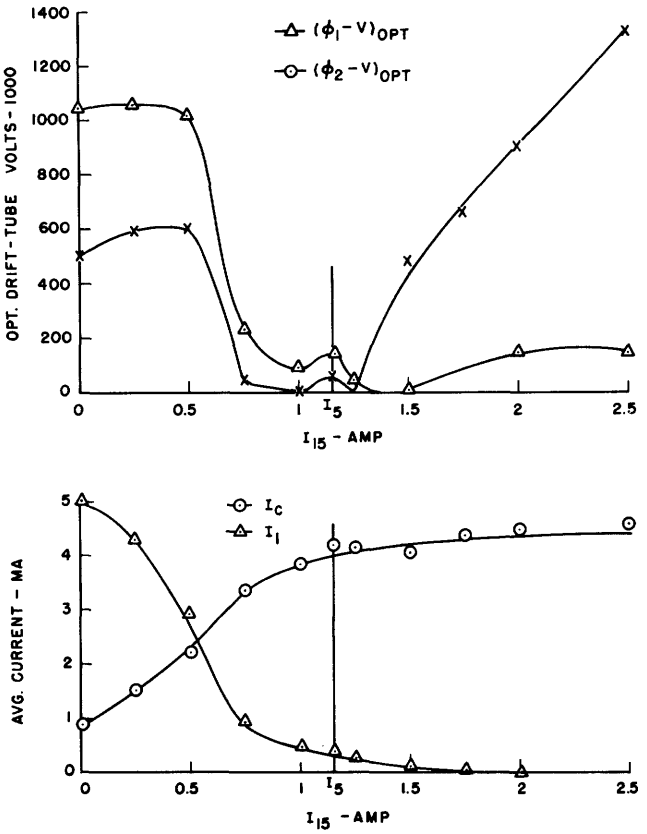

Fig. 33 Optimum voltages as functions of magnetic field configuration, tube No. 2.

of I_{15}, φ_1 is consistently greater than φ_2 for optimum results. As the value of B approaches that of B_c, the average angular velocity decreases in magnitude and φ_1 approaches φ_2. The decrease in angular velocity means a lower energy associated with the rotation so both φ_1 and φ_2 drop to relatively low values above the anode voltage V. For values of I_{15} or B greater than those of I_5 or B_c, the rotation reverses its direction and increases again. This requires a reversal of the potential difference between the drift tubes and an increase of the actual energy level.

When $B = B_c$, a slight inward electric force is necessary to balance the space charge, the cross-over point for $\varphi_2 - \varphi_1$ is therefore at a value of B slightly higher than B_c.

It is interesting too, that the collector current curve is relatively flat for $B > B_c$ and decreases quite definitely at the lower values of I_{15}. The collector current does not become zero with zero magnetic field, a fact which gives us some hope for success of the experiments with the third tube which we are about to consider.

Tubes 3 and 4

The electron gun built with steel parts was intended to satisfy the requirements of a shielded gun as outlined in secs. V and VI. No magnetic field was supposed to penetrate into the anode-cathode region of the gun, and the field across the anode gap due to the gun coil was supposed to be radial. Actually, the structure used fell short of these specifications. The magnetic field across the anode gap fringed out appreciably toward the cathode. This is not surprising as the cathode to anode spacing was of the same order of magnitude as the length of the air gap.

This fringing is shown in the top half of Fig. 34, which is a graph of

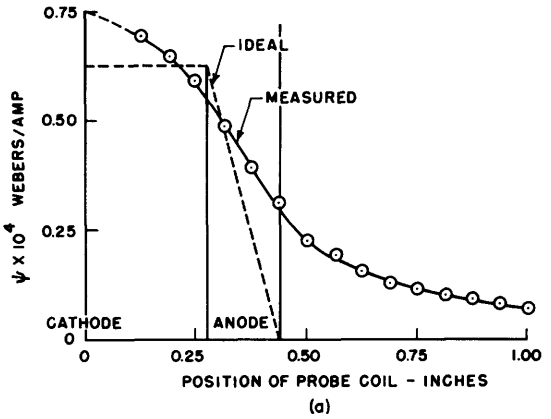

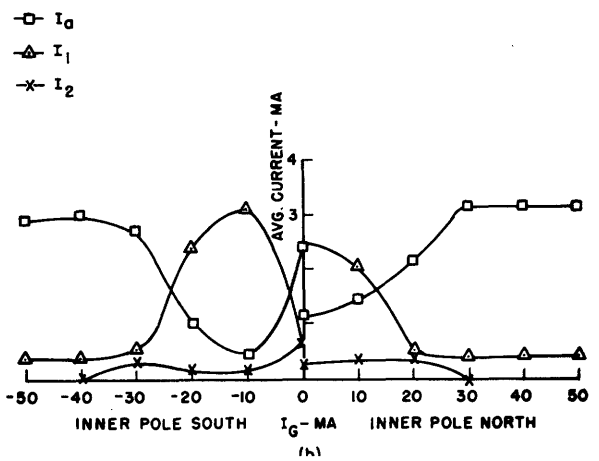

Fig. 34 Characteristics of shielded gun. a. Flux linking outer edge of beam vs. axial position; b. Hysteresis and defocusing due to fringing magnetic field - $I_{1S} = 0$, $I_S = 0$, φ_2 - V = 183 volts, φ_1 - V = 885 volts.

the flux linking a probe coil of radius r_b as a function of the axial position of the coil. If there were no fringing, the curve would be flat behind and in front of the anode and would drop sharply as the anode gap was traversed. The actual flux distribution is seen to be quite different from the ideal.

The effect of the magnetic field distribution on the performance of the gun is a serious one and is shown in the bottom graph of Fig. 34 which also illustrates the hysteresis in the magnetic circuit. The readings for this graph were started at I_G = 0 and went toward the positive side; then I_G was returned to zero, without demagnetizing and increased in the negative direction. The significant feature is the relatively low value of anode current with no magnetic field and its increase with increase of field strength in either direction. The gun, designed for operation in a zero or uniform magnetic field, just does not function properly when there is a field oblique to the cathode.

Fortunately, this fringing field could be compensated by the field of the short solenoid (I_S) placed over the entire gun structure. When this was done, a current through the internal gun coil could be maintained and the beam still brought out past the anode to where it could be focused in the drift tubes. This compensating field had the disadvantage of complicating the flux pattern so that the value of ψ_c could not be measured. The best we can do under these circumstances is to estimate its order of magnitude.

The thicker anode of tube 4 was incorporated in an attempt to reduce the relative importance of the fringing field compared to the total gap flux. In practice, however, the results of experiments on tube 4 were remarkably close

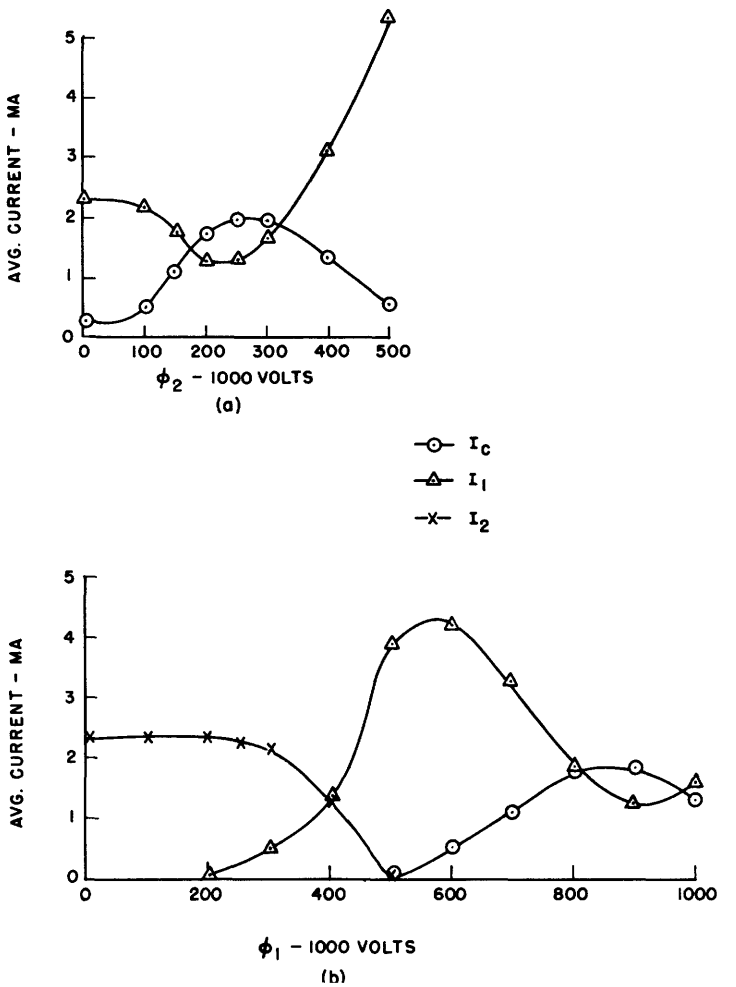

Fig. 35 Focusing as a function of drift-tube voltages, tube No. 3 - $I_{15} = 0$, $I_5 = 0.90$ amp, $I_G = 34$ ma, B = 0.
a. φ_1 - 1000 = 865 volts; b. φ_2 - 1000 = 250 volts.

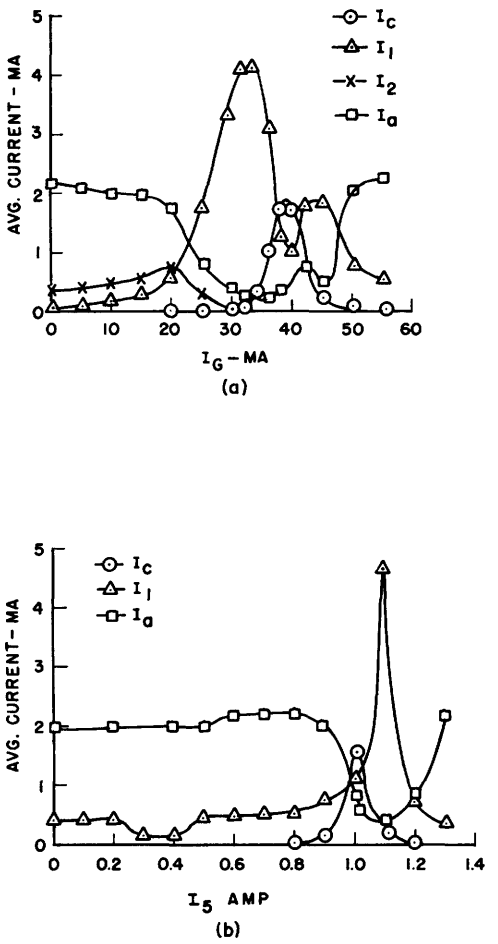

Fig. 36 Focusing with B = 0, tube No. 3.
a. Effect of varying cathode flux - $I_{15} = 0$, $I_5 = 0.90$ amp, φ_1 - V = 865 volts, φ_2 - V = 250 volts.
b. Effect of compensating field - $I_{15} = 0$, $I_G = 36$ ma, φ_1 - V = 865 volts, φ_2 - V = 250 volts.

to those of tube 3 and the curves were confirmed qualitatively down to every undulation. The only observable difference was an increase in the difficulty of balancing out the fringing field and the collector current had somewhat lower maxima than those obtained in the third tube.

The design parameters for the case of focusing with no magnetic field (B = 0) are given below for comparison with the results about to be discussed.

$$\Psi_c = 5.47 \times 10^{-6} \text{ weber}, \quad \varphi_1 = 1885 \text{ volts}, \quad \varphi_2 = 1183 \text{ volts}.$$

Figure 35 shows the effects of varying the drift-tube voltages separately with I_G and I_5 set at optimum values determined experimentally. The important thing about these curves is that they do show an appreciable maximum of collector current proving that this type of focusing is possible. The optimum drift-tube voltages, moreover, are in reasonable agreement with the theoretical values. The results of tube 4, not shown here, are in even closer agreement with the theory, the optimum value of φ_1 being 1870 volts and that of φ_2, 1175 volts. The value of ψ_c calculated from the observed value of I_G and the calibration curve at the top of Fig. 34 and neglecting the compensating field is about 3×10^{-8} weber which is about as close as we could judge with this arrangement.

Figure 36 shows the effects of varying the value of ψ_c and the compensating field separately. The compensation is shown in both graphs by the dips in anode current while the criticalness of the actual values of ψ_c are shown by the sharp peaks in collector current.

In each of the curves of the last two figures, large maxima of inner drift-tube current are apparent and these require explanation. Judging from the results of the tests on tubes 1 and 2, we should expect I_1 to decrease continuously as φ_2 is increased or to increase as φ_1 is increased. Reference to Fig. 35 shows that this is not the case. The explanation of this anomalous behavior is in the effects of secondary emission. It is not shown on the graphs but the outer drift-tube current was negative for many of the settings used in taking these curves. This is evidenced by the sharp drop in I_2 in the lower curve of Fig. 35. Actually this line continued on to negative values.

For secondary emission from the outer drift tube with a ratio greater than one, the result is an effective flow of electrons from outer to inner drift tube. The secondary emission ratio changes value with the angle of incidence of the primaries, increasing sharply as the primaries graze the surface (ref. 18). The observed effects, therefore, depend on the focusing conditions.

This effect is quite pronounced in this tube and not in tubes 1 or 2 because of the absence of the main magnetic field. Low-velocity secondary electrons liberated in a magnetic field would just loop around without crossing the tube (see sec. VII), but when the field is absent, there is no reason for the secondaries not to move toward the higher potential electrode. This behavior could be an argument against this type of focusing in certain cases.

It should be remembered too, that the charge distribution in these beams is heavily concentrated toward the inside. In all cases the inner drift-tube current was much more apparent than that going to the outer tube.

The final curve shown here, Fig. 37, illustrates the possibility of focusing with no applied potential difference between the drift tubes. A magnetic field over the drift-tube region was used in this case. It is

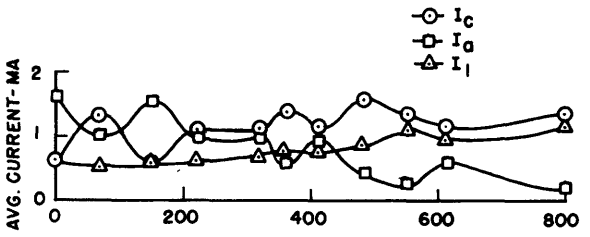

Fig. 37 Focusing with $\varphi_1 = \varphi_2$ - $I_{15} = 1.61$ amp, $I_5 = 0$, $I_G = -13$ ma.

interesting that the collector and anode current curves are almost mirror images, illustrating once more that the focusing is alright if the beam can be brought through the transition region. The transition region in this case lies in the anode gap.

This discussion completes the experimental work done on the problem and in the next section some conclusions are drawn and suggestions made for extension of this work.

X. CONCLUSIONS

The foregoing discussion of the experiments bears out the remarks made previously about their interpretation. It is clear that the tests are not as clean-cut as would be desirable, in that the separation of the various factors affecting the performance was not possible. Before we can draw positive conclusions about the theory a more extensive and careful experimental program will have to be carried out.

It does appear, however, that the qualitative aspects of the theory are very well confirmed by the experimental results, and the indications are that the quantitative aspects are confirmed reasonably well. In every case where the experiments were not successful, the cause of the failure could be attributed with fairness to the transition region. We may conclude, therefore, that the theory as presented is substantially correct as far as it goes.

A particular advantage of the analysis as presented is that the magnetic field effects are expressed in terms of flux linkages. This integrated quantity is easy to calculate or measure by mutual inductance methods, particularly in axially symmetric systems.

Little light has been shed on the question of whether the assumption of noncrossing is a valid one, but apparently it is either largely true or makes little difference anyway, probably the latter. For purposes of computation at least, it is relatively safe to make this assumption.

The design formulae presented in this paper are essentially correct and useful as they stand, though they do not provide one with complete design data for a hollow electron beam system. Only the uniform part of the system can be designed with confidence. Electron guns are easily designed also, but their coordination with the rest of the system has not been completely specified.

For the uniform part of the system, the actual drift-tube voltages and

magnetic field strengths are not very critical, but the magnetic field configuration and cathode flux condition must be set quite accurately. This condition (Eq. 27) is probably the most important one to come out of the analysis.

Although there seemed to be some indication that residual gas ionization partially neutralized the space charge of the beam, the results were so indefinite that no definite conclusions can be drawn from them in this respect. The discussion of sec. VII must remain as it was presented, merely an exposition of various possibilities with little attempt to predict their relative probabilities.

The feasibility of focusing in any of the special cases of sec. VI has been demonstrated. Noteworthy among these is the case where the magnetic field is required in the cathode region only, because of its practical significance in the economy of magnetic field and simplification of the entire beam system. This focusing system may well be a good reason in itself to use hollow beams in place of solid ones.

Before this case can be applied in general practice, however, an improved design over that used here should be developed. A further separation of the electron gun and magnetic circuits is indicated. If the magnetic air gap were placed well forward of the anode of the gun, fringing in the region of the cathode could be reduced to negligible amounts. For smaller tubes it would be feasible to close the magnetic circuit linking the electron gun, and to activate this circuit, outside the vacuum envelope on the tube. Kovar to glass seals could be used advantageously here.

A considerable part of the value of this investigation may lie in the various problems it suggests. The chief and most obvious of these is the problem of the transition region.

This subject will have to be investigated more thoroughly before the results of the analysis in the present paper can be put to efficient use. If there is one point emphasized by the experimental results, it is the necessity for a good transition region design. Two approaches to this problem may be taken. The electron trajectories may be assumed and the design conditions derived from these, as was indicated in this paper; or the electron paths may be calculated for a set of known conditions and the electron gun then placed in the appropriate position.

There is no need to restrict the problem to those cases presented here. These restrictions were imposed for the sake of simplicity but there is no necessity for them. Undoubtedly there are many other cathode arrangements susceptible to analysis and perhaps more convenient. One such example is the cylindrical cathode proposed by Brillouin (ref. 8) which falls in the category of ψ_c the same for all electrons, if it is immersed in a uniform axial

field. A survey of possible cathode and electron gun configurations might be a very profitable endeavor.

In addition to the immediate problems arising in this work, there are others which must eventually come to the fore as these beams are put to use.

Assuming that one of the principal uses of hollow beams is to be in high-power microwave tubes, two questions come to mind. The first is: What effect will the radio-frequency fields and bunching have on the dynamics of these beams? Some consideration has already been given to this problem for the case of solid beams (ref. 7). The second question is: How is the amplification process in traveling-wave or electron-wave tubes affected by the helical flow in these beams? This question will probably be of particular importance in connection with helix type traveling-wave tubes.

In the opinion of the author, the two main benefits derived from this investigation are the increased general understanding of the focusing of electron beams by magnetic fields and the emphasis on the problem of bringing the beam through the nonuniform part of the magnetic field. Previously, with the general use of solid beams, the beam system and electron gun could be designed independently and operated together with good assurance of success. This success is due to some extent to the fortuitous circumstance that the proper focusing condition for solid beams is to have the cathode outside the magnetic field. With small diameter beams, the transition region could be made short and the beam passed through.

When hollow beams are used the focusing conditions are more stringent as both inner and outer radii must be controlled. The transition region problem cannot be avoided as it is generally necessary to have some flux link the cathode, and unless the gun is shielded, this region is of appreciable length.

The success of the experiments and theory is probably best shown by the fact that in tubes 1 and 2, the beam was focused with no loss to the drift tubes by magnetic fields of only 100 to 150 gauss density. In tube 3, a substantial focusing effect was obtained with a very much smaller total magnetic flux.

APPENDIX I. VARIATIONAL TREATMENT OF THE EQUILIBRIUM CONDITIONS

In this appendix it is shown by means of variational treatment of the problem that any radial charge distribution in the beam is a stable configuration so long as the proper conditions on the magnetic flux are satisfied. The coordinates, symbols and assumptions used here are the same as those of sec. II.

The conditions we are seeking here are equilibrium conditions only. The beam is taken as perfectly uniform longitudinally with no radial oscillations

of the electrons allowed. We consider the entire beam as a unit with a radial charge distribution ρ between the radii r_a and r_b. The problem is to find a potential distribution $\varphi(r)$ such that the assumed beam will be in stable equilibrium.

The condition for stable equilibrium of any dynamical system is that the total potential energy of the system be a minimum. In this statement we must be careful as to just what the potential energy is. We define it by the relation

$$\text{Potential Energy } (\eta) + \text{Kinetic Energy } (\nu) = \text{a constant } (A) \; . \tag{A-1}$$

The only motion that disturbs the equilibrium we are considering is that in the radial direction, so the kinetic energy is that associated with radial motion.

$$\nu = \frac{m}{2} \dot{r}^2 \; . \tag{A-2}$$

The potential energy consists, therefore, of all the other terms, including what we ordinarily call the kinetic energies associated with axial and tangential motions. For one electron the potential energy is

$$\eta = A - \nu = A - \frac{m}{2} \dot{r}^2 \; . \tag{A-3}$$

The potential energy of the entire beam of electrons is the sum of all the η's, provided each η is calculated taking into account the presence of all the other electrons, i.e. we do not neglect the space charge.

From (22) and by retaining φ in its original form rather than $\alpha \ln r/r_o + \gamma$ we have

$$\dot{r}^2 = -2 \frac{e}{m} (\varphi - V) - \frac{\Omega^2}{r^2} - \omega_H{}^2 r^2 + 2\omega_H \Omega \tag{A-4}$$

where

$$\Omega = \frac{e}{m} \frac{\psi_c}{2\pi} \qquad\qquad \omega_H = \frac{e}{m} \frac{B}{2} \; .$$

Equation A-3 becomes

$$\eta = A + e(\varphi - V) + \frac{m}{2} \frac{\Omega^2}{r^2} - m\Omega\omega_H + \frac{m}{2} \omega_H{}^2 r^2 \; . \tag{A-5}$$

The total number of electrons per unit length of a shell between radii r and r + dr is $2\pi\, r\, \rho/e\, dr$ and the potential energy dH of this shell is

$$dH = 2\pi\, r\, \eta \frac{\rho}{e} dr \; . \tag{A-6}$$

The total potential energy of the entire beam per unit length is the integral of (A-6)

$$H = \int_{r_a}^{r_b} 2\, \pi\, r\, \eta\, \frac{\rho}{e} dr \; . \tag{A-7}$$

But ρ is related to φ through Poisson's equation

$$\rho = -\varepsilon \nabla^2 \varphi = -\varepsilon \left(\frac{\partial^2 \varphi}{\partial r^2} + \frac{1}{r} \frac{\partial \varphi}{\partial r} \right) . \tag{A-8}$$

We require ρ, hence $\nabla^2 \varphi$, to be zero inside and at r_a, and outside and at r_b. With (A-8) and (A-5) substituted into (A-7), it becomes

$$H = -\frac{2\pi\varepsilon}{e} \int_{r_a}^{r_b} \left(\varphi'' + \frac{1}{r} \varphi' \right) r \left[A + e(\varphi - V) + \frac{m}{2} \frac{\Omega^2}{r^2} - m\omega_H \Omega + \frac{m}{2} \omega_H^2 r^2 \right] dr \tag{A-9}$$

where

$$\varphi'' = \frac{\partial^2 \varphi}{\partial r^2} \qquad \varphi' = \frac{\partial \varphi}{\partial r}$$

Equation A-9 may be written in a shorter form

$$H = -\frac{2\pi\varepsilon}{e} \int_{r_a}^{r_b} F(\varphi, \varphi', \varphi'') dr . \tag{A-10}$$

Since we are seeking the function φ which will minimize this integral, we have a typical problem in the calculus of variations. The condition that H be an extreme value is given by the Euler equation (ref. 19),

$$\frac{\partial F}{\partial \varphi} - \frac{d}{dr} \left(\frac{\partial F}{\partial \varphi'} \right) + \frac{d^2}{dr^2} \left(\frac{\partial F}{\partial \varphi''} \right) = 0 . \tag{A-11}$$

From this point on, the computations are quite mechanical. They consist of taking the derivatives of F, (the integrand of (A-9)) indicated by (A-11) and evaluating the left-hand side of (A-11). In this process Ω is considered as a regular single-valued function of r, and of course ω_H and V are constants. This treatment of Ω is equivalent to the assumption of no radial crossing. If electrons did cross them at some radii, there would be two or more values of Ω corresponding to the separate values of ψ_c of each of the electrons at that radius.

If the left-hand side of (A-11) is computed as indicated above, it is found that it simplifies to

$$\frac{\partial F}{\partial \varphi} - \frac{d}{dr} \left(\frac{\partial F}{\partial \varphi'} \right) + \frac{d^2}{dr^2} \left(\frac{\partial F}{\partial \varphi''} \right) = \frac{\partial}{\partial r} r \frac{\partial}{\partial r} \left[2\varphi + \frac{m}{2e} \left(\frac{\Omega}{r} - \omega_H r \right)^2 \right] \tag{A-12}$$

According to (A-11) this should be zero, so the stability condition is

$$\frac{\partial}{\partial r} r \frac{\partial}{\partial r} [\zeta] = r \nabla^2 \zeta = 0 \tag{A-13}$$

where

$$\zeta = 2\varphi + \frac{m}{2e} \left(\frac{\Omega}{r} - \omega_H r \right)^2 . \tag{A-14}$$

Equation A-13 is merely Laplace's equation with ζ playing the role usually occupied by the potential. If we had solved any electrostatic problem in a charge-free region by the method we have used here, we would have arrived at

Laplace's equation

$$\nabla^2 \varphi = 0 \ . \qquad \text{(A-15)}$$

We may conclude that ζ is a potential function derived from the magnetic field conditions and which effectively eliminates the effects of space charge. It is now clear that φ and hence ρ may be any functions of r at all and still satisfy the equilibrium conditions, so long as Ω can be adjusted to satisfy (A-13).

It is not surprising to note by referring to (42) that the second term of ζ is merely $m/2\ (r\dot{\theta})^2$

$$\zeta = 2\varphi + \frac{m}{2e}(r\dot{\theta})^2 \qquad \text{(A-16)}$$

i.e. ζ is a potential function consisting of the electric potential energy associated with φ plus the energy associated with the angular velocity. This is what we should expect in view of our method of setting up the problem, and the comments following Eq. 22.

The conclusions outlined above confirm the ideas put forward in sec. II. This variational treatment does not actually give us any more information than we obtained by our first method and appears to be considerably more involved, so it has not been pursued as a method of complete solution, as it might have been. It is included here in the hope that the alternative viewpoint clarifies the nature of the problem and the assumptions that have been made.

APPENDIX II. CALCULATION AND MEASUREMENT OF THE MAGNETIC FIELD

A detailed knowledge of the magnetic field configuration is necessary in the transition region if we are to design the proper system as outlined in sec. V. Since the entire analysis is carried out in terms of flux linkages, it is advisable to keep any determination of the magnetic field in this form. The problem of measurement then becomes a very simple one as we need only to measure the mutual inductance between the field coil and a thin probe coil. Relative measurements are easily obtained and a single calibrating measurement serves to set all of these on an absolute scale.

Figure A.1 shows a device built for the measurement of the field coils used in this report. In the face of this tube there is a set of thin coils of fine wire. Each coil has 50 turns and they all lie in the same plane at right angles to the axis. The mutual inductance measurement with this device is so simple it needs no further explanation. Care must be taken to orient the tube so that the pickup in the leads is as small as possible. This means the terminals should lie farther from the solenoid than the measuring coils themselves.

Figures A.2 and A.3 show the results of these measurements compared with

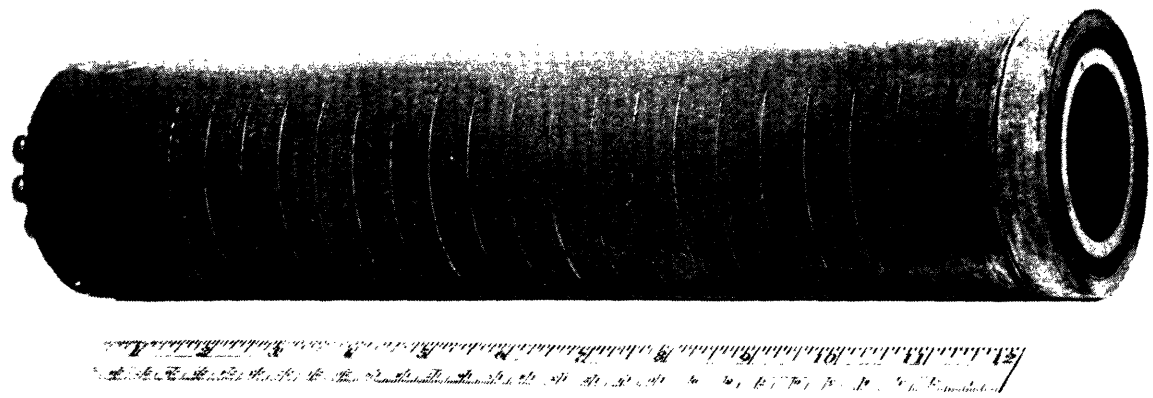

Fig. A.1 Tube with probe coils.

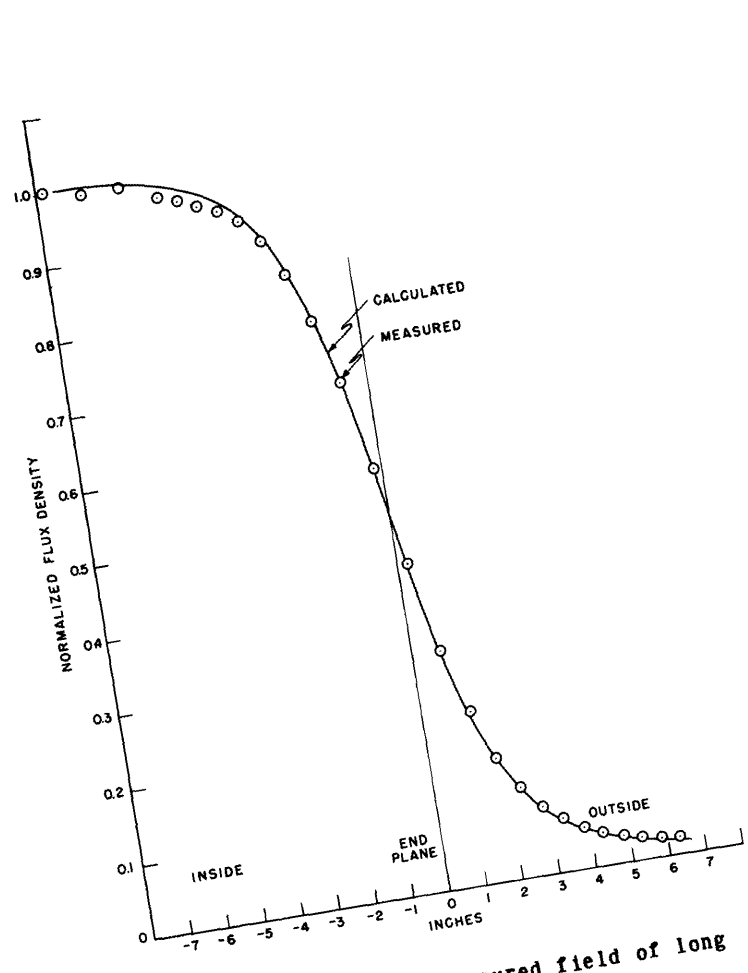

Fig. A.2 Calculated and measured field of long solenoid.

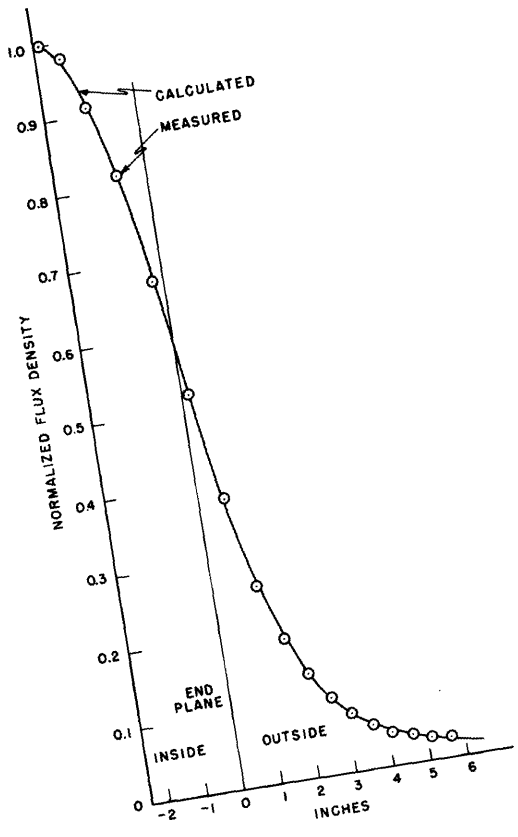

Fig. A.3 Calculated and measured field of short solenoid.

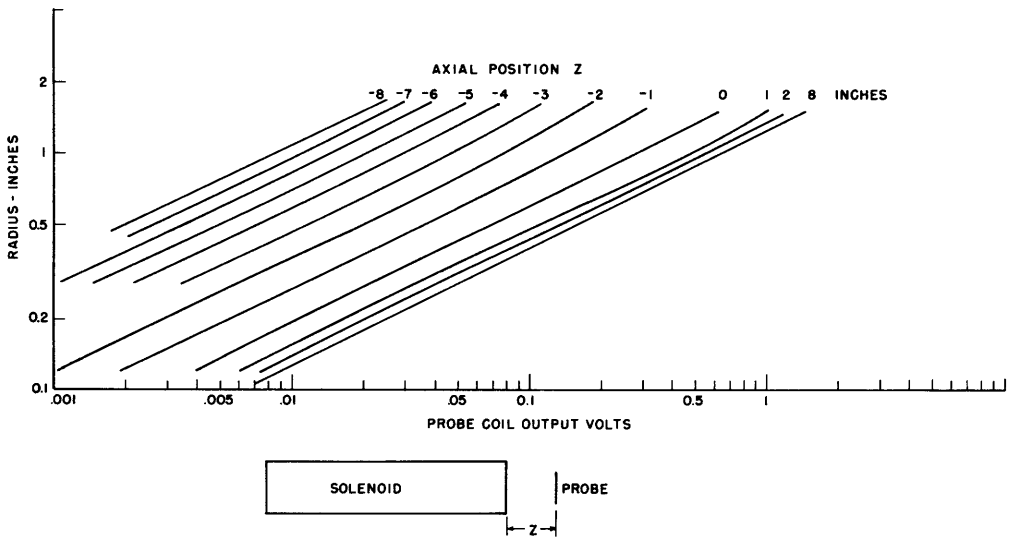

Fig. A.4 Radius *versus* flux linkage in the long solenoid.

the calculated curves. The curves are normalized so that the resultant magnetic field of the two coils together may be determined by proper scaling and superposition.

The calculation of Magnetic fields of solenoids of various dimensions may be carried out by the use of mutual inductance formulae found in many books and papers on the subject. For thin solenoids without iron, the calculations are conveniently done by use of the formulae and table given in chapter 14 of "Inductance Calculations" by F. W. Grover (ref. 20).

Figure A.4 is a log-log plot of radius versus output voltage obtained from the same measurements used to plot the normalized curves in Figs. A.2 and A.3. The fact that all these curves are very close to straight lines of slope equal to one half proves the statement made previously that in any cross-sectional plane the flux ψ is proportional to r^2. Because of this, ψ may be represented by

$$\psi = \pi r^2 B_z$$

where B_z is a function of z only.

ACKNOWLEDGMENT

I wish to express my sincere gratitude to Prof. L. J. Chu, for his wise and patient guidance and constant encouragement, to Mr. L. D. Smullin, for many valuable discussions and suggestions, and to Professors S. T. Martin and J. E. Thomas, Jr., for their interest and suggestions. I am indebted to the many technicians and machinists whose cooperation made the experimental part of this work possible. Particular thanks go to Mr. F. O. Iantosca and Mr. J. B. Keefe for their help in many emergencies.

REFERENCES

1. L. M. Field: Proc. I.R.E. 37, pp. 34-39, 1949.
2. E. E. Watson: Phi. Mag. Ser. 7, 3, pp. 849-853, 1927.
3. B. J. Thompson and L. B. Headrick: Proc. I.R.E. 28, pp. 318-324, 1940.
4. L. T. Smith and P. L. Hartman: Jour. App. Phys. 11, pp. 220-229, 1940.
5. N. Wax: Jour. App. Phys. 20, pp. 242-247, 1949.
6. J. R. Pierce: Proc. I.R.E. 35, pp. 111-123, 1947.
7. R. Berterottiere: Ann. de Radioelect. 4, pp. 289-294, 1949.
8. L. Brillouin: Phys. Rev. Ser. 2, 67, pp. 260-266, 1945.
9. L. M. Field: Rev. Mod. Phys. 18, pp. 353-361, 1946.
10. C. C. Wang: Proc. I.R.E. 38, pp. 135-147, 1950.
11. A. L. Samuel: Proc. I.R.E. 37, pp. 1252-1258, 1949.
12. P. Bergmann: Introduction to the Theory of Relativity, Ch. 7, pp. 106-120
13. J. R. Pierce: Theory and Design of Electron Beams, Ch. 4, p. 35, D. Van Nostrand Co., Inc., 1949.
14. J. R. Pierce: Theory and Design of Electron Beams, Ch. 10, pp. 167-186, D. Van Nostrand Co., Inc., 1949.
15. K. R. Spangenberg: Vacuum Tubes, Ch. 15, pp. 440-465, McGraw-Hill Book Co., Inc., 1948.
16. R. Q. Twiss: Doctoral Thesis, Physics, M.I.T., Ch. 4, 1949.
17. R. Musson-Genon: Ann. de Telecomm. 2, pp. 254-320, 1947.
18. K. R. Spangenberg: Vacuum Tubes, Ch. 4, p. 54, McGraw-Hill Book Co., Inc., 1948.
19. P. Franklin: Methods of Advanced Calculus, Ch. 12, p. 432, McGraw-Hill Book Co., Inc., 1944.
20. F. W. Grover: Inductance Calculations, Ch. 14, pp. 114-119, D. Van Nostrand Co., Inc., 1946.